

Investigating the Feasibility of Deploying Scalable Ad-Hoc DC Microgrids for Rural Electrification Through Hardware and Software Techniques



Didier Iradukunda

Supervisor

Prof. Willem Cronje

May 2018

Submitted to the School of Electrical and Information Engineering of the University of the Witwatersrand in fulfilment of the requirements for a Masters of Science degree in Electrical Engineering.

Abstract

This dissertation investigates the technical feasibility of deploying scalable hybrid DC picogrid systems for rural off-grid areas, by assessing the technical (hardware and software) requirements for implementing a minimal (12V, 100W nominal), laboratory prototype of such a system. The laboratory prototype validates the proposed concept of an ad-hoc localised low-voltage DC grid (“Picogrid”) as a resilient and robust solution for off-grid electrification at low power levels. It demonstrates the scalability, fault tolerance and other features which are required for the intended application.

Existing off-grid low voltage DC systems (like the solar home systems) cannot be scaled up in terms of power increase, load expansion or storage extension and this severely limits the usability of the available systems. The “Picogrid” concept put forward here is one of the possible solutions that can be scaled in every dimension (generation, storage and load) by having multiple autonomous sources and storage nodes networked together in an Ad-Hoc manner. Stable operation is achieved by a global grid code defining each node’s action based on the state of the bus voltage as opposed to the state of other nodes. A decentralized form of droop control that applies proportional control of voltage and current was implemented on four prototype nodes with each controller’s decision based on the state of the picogrid bus voltage.

Individual node and overall system tests were performed on the prototype. Node tests include; open circuit, short circuit, current limit, over voltage, under voltage and effects of suddenly removing a heavy load. Sharp voltage spikes were observed when a load is suddenly disconnected from the grid due to the sudden drop of load current. These spikes were minimized by having controllers tripping the nodes immediately when the bus voltage rises. Apart from recommending future hardware improvements to the power supply circuit, A different control platform that processes faster than the one used for the picogrid was recommended in order to completely eliminate the spikes. The ease of power scaling as well as recovering from faults without requiring any user interaction was illustrated through system tests when all nodes were connected together. This further proves the picogrid to be a feasible technical solution that can be extended to a full commercial application. Furthermore, the tests show that by having more sources or storage nodes, more power can be automatically obtained from the system. The maximum power produced by a picogrid system

is however limited to the hardware composition especially with regards to the node-node connector cables. Thus the cable size used will determine the maximum power of the system for deployment purposes when costs need to be taken into consideration.

Declaration

I declare that this dissertation is entirely my own unaided work and that any material regarded as the work of others has been cited and referenced. It is being submitted for the degree of Masters of Science in Electrical Engineering.

Signature:

Name of student: Didier Iradukunda

Date:

Acknowledgements

It is with great honour to have this opportunity to express my gratitude to all the people that assisted, influenced and supported my work directly or indirectly. A Special thanks to my supervisor, Professor Willem Cronje for steering such an interesting research and equipping me with the necessary skills in this particular field of renewable energy.

I would also like to thank Doctor Wesley Doorsamy for the technical support and insight into the research that made all of this possible.

A special thanks to Doctor Shuma-Iwisi for the positive feedback and steering me to conducting a fruitful research.

To my entire family, thank you for the continuous and relentless support throughout my undergraduate and postgraduate studies.

I would also like to extend my gratitude to my colleagues, team mates, work mates, brothers and sisters of Thusanani Foundation and Lamo Solar for providing the selfless support not only to me but to all students across South Africa who graduate as “solid graduates,” that is, graduates with low self-esteem and high group esteem that enables them to give back to their communities.

And finally, I would like to thank Nthabiseng Mohale for the mental and physical support she showed me throughout the entire research process. Thank you very much for always being available. I will forever be grateful.

Acronyms

A	Ampere
CCM	Current Control Mode
DB	Data Block
DBS	DC Bus Signalling
DRES	Decentralised Rural Electrification Systems
DCBC	Direct Current Bus Control
FB	Function Block
HMI	Human Machine Interface
IEA	International Energy Agency
IPP	Independent Power Producer
LSM	Living Scale Mechanism
LED	Light Emitting Diode
LVDC	Low Voltage Direct Current
MPPT	Maximum Power Point Tracking
OB	Organisation Block
OC	Open Circuit
PCB	Printed Circuit Board
PBV	Picogrid Bus Voltage
PLC	Programmable Logic Controller
PPS	Pico PV Systems
PWM	Pulse Width Modulation
RES	Renewable Energy Storage
SC	Short Circuit
SHS	Solar Home System
SoC	State of Charge
SMPS	Switch Mode Power Supply
TIA	Totally Integrated Automation
VCM	Voltage Control Mode
WEO	World Energy Outlook

Table of Contents

Abstract.....	i
Declaration.....	iii
Acknowledgements	iv
Acronyms	v
Table of Contents	vi
List of Figures.....	ix
List of Tables	xi
1. Introduction	1
1.1. Objective and Requirements	1
1.2. Research Methodology.....	3
1.3. Problem Statement	4
1.4. Research Question.....	5
1.5. Scope and Limitations.....	5
1.6. Report Outline	5
2. Background	7
2.1. Global Access to Energy	7
2.2. Access to Energy in Africa.....	7
2.3. Africa's Energy Consumption per Capita versus Carbon Dioxide Emissions.....	8
2.4. Summary	10
3. LVDC Systems for Rural Areas	11
3.1. Introduction	11
3.2. Single-Source, Single-Storage and Single-Load systems	11
3.3. Single-Source, Single-Storage, Multiple-Load Systems.....	12
3.4. Single-Source, Multiple-Storage, Multiple-Load Systems	13
3.5. Multiple-Source, Multiple-Load and Single-Storage Systems	14
3.6. Pre-Paid Solar Home Systems.....	15
3.7. Stand-Alone DC Microgrids	15
3.8. Droop Control of LVDC systems	16
3.9. Summary	16
4. Picogrid Structure and Operation	18
4.1. Introduction	18
4.2. Picogrid Structure.....	18
4.3. Picogrid Operation	19
4.3.1. Grid Code.....	19
4.3.2. Picogrid Bus Voltage	21

4.3.3.	Scalability	22
4.3.4.	Stability	22
4.3.5.	Protection	23
4.4.	Summary	23
5.	Picogrid Implementation	24
5.1.	Introduction	24
5.2.	Node Structure.....	24
5.2.1.	Source Nodes	24
5.2.2.	Storage Node.....	26
5.2.3.	Load Node.....	27
5.3.	Node Components.....	28
5.3.1.	Flyback Converter Circuit.....	28
5.3.2.	Controller	31
5.3.3.	24 VDC Power Supply.....	32
5.3.4.	24V-12V DC Regulators.....	32
5.3.5.	PBV Indicator LEDs	32
5.3.6.	Solar/ Wind Regulator Knobs.....	33
5.4.	Other Required Components	34
5.4.1.	HMI Display Panel	34
5.4.2.	Network Switch	34
5.5.	Summary	35
6.	Control System and Protection	36
6.1.	Introduction	36
6.2.	Control Structure Overview	36
6.3.	Common Control Algorithm	37
6.4.	Solar and Wind Node Control.....	38
6.4.1.	Primary and Secondary Control Algorithms.....	38
6.4.2.	Tertiary Control Algorithm.....	39
6.5.	Load Node Control.....	40
6.5.1.	Tertiary Control Algorithm.....	41
6.6.	Storage Node Control.....	42
6.6.1.	Primary and Secondary Control Algorithm	42
6.6.2.	Tertiary Control Algorithms	43
6.7.	Summary	45
7.	Picogrid Tests and Results	46
7.1.	Introduction	46
7.2.	Test Setup	46

7.3.	Node Tests.....	47
7.3.1.	Open Circuit Voltage and Short Circuit Current tests with no load	47
7.3.2.	Under Voltage and Over Voltage tests	50
7.3.3.	Load tests on Individual Nodes.....	50
7.3.4.	Load Shedding test.....	56
7.3.5.	Sudden Removal or Connection of Load.....	60
7.4.	System Tests.....	62
7.4.1.	Load Located on Load Node.....	63
7.4.2.	Storage Node test	65
7.5.	Summary	67
8.	Conclusion and Recommendations	68
8.1.	Conclusion.....	68
8.1.1.	Research Question	69
8.2.	Future work Recommendations	70
8.2.1.	Hardware Improvements.....	70
8.2.2.	Software Improvement.....	71
8.2.3.	Further Tests	71
References.....		74
Appendices.....		77

List of Figures

Figure 1: Hybrid DC Picogrid.....	2
Figure 2: Research methodology flowchart	4
Figure 3: The LSM triangles of sub-Saharan Africa population showing; (a) Urban and Rural Population versus (b) Energy consumption per capita	8
Figure 4: Global energy consumption by source [6]	9
Figure 5: Global Carbon Dioxide emissions vs Energy per Capita (kWh/Person).	10
Figure 6: Solar light structure	11
Figure 7: A Solar Home System structure with multiple nodes	12
Figure 8: Schneider Solar Home System	13
Figure 9: Two Pico lamps connected together for power sharing	14
Figure 10: Sharetech hybrid system structure [26]	15
Figure 11: A Stand Alone DC Microgrid structure	16
Figure 12: Hybrid DC Picogrid.....	19
Figure 13: Picogrid Bus Voltage (PBV) code.....	20
Figure 14: Node operation flow chart.....	22
Figure 15: Solar node photograph.....	25
Figure 16: Power and information flow between components of source nodes (solar and wind)	25
Figure 17: Storage node photograph.....	26
Figure 18: Power and information flow between components of a storage node.....	26
Figure 19: Load node picture	27
Figure 20: Load node power and information flow block diagram	27
Figure 21: Flyback converter showing VCM and CCM regions	30
Figure 22: PLC functional block diagram	31
Figure 23: PBV LEDs connection to PLC relays	33
Figure 24: Solar/Wind regulator Knob	33
Figure 25: Star topology network connection between PLCs, HMI and host computer	34
Figure 26: Picogrid Star topology network picture.....	35
Figure 27: Control system structure of a source and storage node	37
Figure 28: PBV LED indicator Algorithm.....	38
Figure 29: Source node control blocks	39
Figure 30: Tertiary control flow chart algorithm	40
Figure 31: Load shedding concept.....	41
Figure 32: Load node control Algorithm	42
Figure 33: Storage node control blocks	44
Figure 34: Storage node control algorithm process flowchart.....	45
Figure 35: Picogrid laboratory test setup	46
Figure 36: OC and SC test setup diagram for; (a) wind, (b) storage and (c) solar node	47
Figure 37: Wind node OC voltage versus SC current, OV and UV tests	48
Figure 38: Solar node OC voltage versus SC current	49
Figure 39: Storage node OC voltage versus SC current	49
Figure 40: Load tests setup for each node	51
Figure 41: Wind node voltage and current waveforms against time, with a varying load	51
Figure 42: Wind node voltage versus current graph of the varying load.....	52
Figure 43: Solar node voltage and current graphs of a varying load	53
Figure 44: Solar node voltage versus current graph of the varying load	54

Figure 45: Storage node voltage and current graphs of a varying load	55
Figure 46: Storage node voltage versus current graph of the varying load	55
Figure 47: Load shedding test setup	57
Figure 48: Non-conditional load profile	58
Figure 49: Conditional load profile.....	58
Figure 50: Load shedding test results	59
Figure 51: Zoom in at the 1 st load shedding of figure 50	60
Figure 52: Voltage and Current versus time when a sudden connection/ removal of load occurs on Storage node	61
Figure 53: Solar node Voltage and Current versus time from sudden connection/ removal of load.....	61
Figure 54: Wind node Voltage and load current versus time from sudden connection/ removal of load	62
Figure 55: System test setup showing four test cases on four nodes	63
Figure 56: voltages and currents graphs versus time for case 1(on wind node) and case 2 (on load node).....	63
Figure 57: voltage versus current for case 1 and case 2	64
Figure 58: Picogrid voltage versus load current showing how scalability is achieved with additional sources or storage nodes	65
Figure 59: Storage node test setup with two sources	66
Figure 60: Storage node voltage and current versus time.....	66
Figure 61: A Picogrid showing limitations with cable properties	71
Figure 62: Graph theorem topology approach	72
Figure 63: Artificial grid structure.....	72

List of Tables

Table 1: Summary of the location and power capacity of different SHS in sub-Saharan Africa	13
Table 2: Node structural components	18
Table 3: Improved flyback converter versions showing major improvements for each node	28
Table 4: Technical specifications of old versus Improved flyback converter circuit	30
Table 5: Node voltage, current and power ratings	56
Table 6: System voltage, current and power ratings of combined two sources and one storage node different cases with varying load	65

1. Introduction

1.1. Objective and Requirements

The main objective of the research is to investigate whether the concept of a scalable Hybrid DC Picogrid can be applied to a prototype for deployment to rural communities. This can only be achieved by first identifying the required fields making up a scalable picogrid. A scalable picogrid should be easily acquired as a small sized system which can be scaled up/down depending on the load requirements. The scaling up/down of the system should be autonomous in a simple “plug and play” manner and user friendly without requesting any information from the user who is considered to be from a rural background. The Picogrid would thus have to meet the following requirements so as to allow for the next phase of deploying the system to the market;

- Construction of four prototype nodes; solar, wind, storage and load nodes.
- Control system setup
- Implementation of Protection schemes
- Hardware and software tests
- Testing of each node
- Perform overall system tests

This research thus proposes a scalable Ad Hoc picogrid as a suitable solution for rural electrification by looking into the unique properties and elements of such a system. There is no specific description classifying picogrids within a particular power range but what is clear is that Picogrids resemble scaled down independent Microgrids [1-2]. A Picogrid can be composed of any number of storage, wind, solar and load nodes. It is termed hybrid DC as it makes use of different sources and operates on a nominal DC voltage and power of 12V and 200W respectively. As shown in figure 1, a Picogrid is formed when a load is connected to either a storage or a source node.

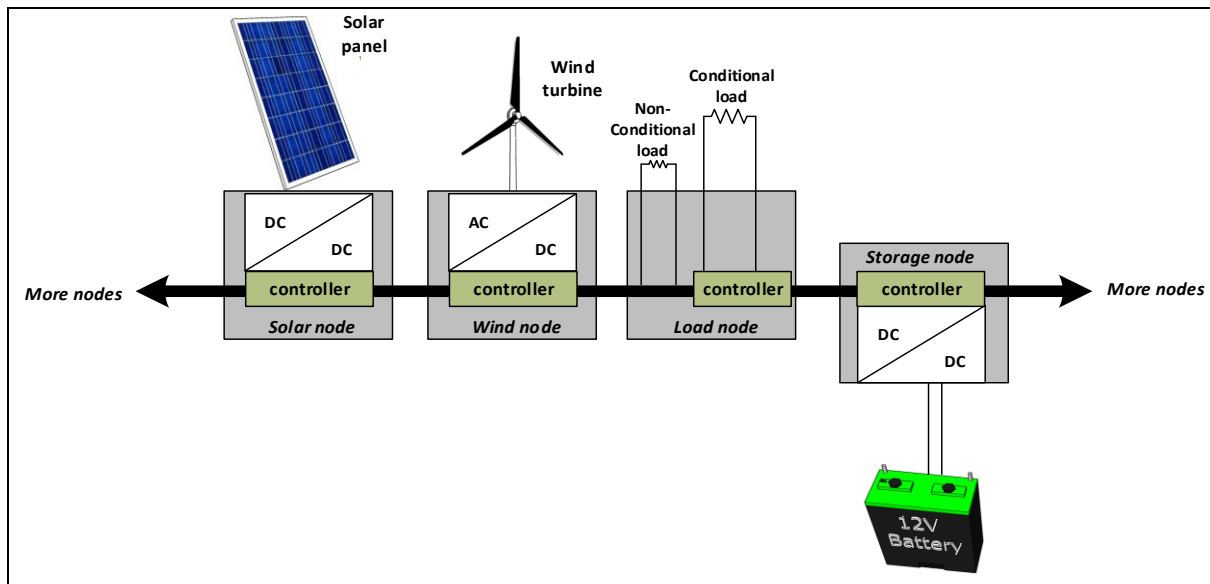


Figure 1: Hybrid DC Picogrid

A key feature of the Picogrid lies in its Ad Hoc property that allows for power scaling in order to meet load demands of a typical rural household. The process of power scaling is made easy through the addition of more sources or storage nodes in a “*plug and play*” manner. As shown in figure 1, each node is autonomous and applies a decentralised control scheme, meaning that its decision making lies on the state of the Picogrid Bus Voltage (PBV) and not on the state of other nodes. The picogrid concept thus resembles that of the national utility grid by being able to incorporate a mixture of different autonomous sources and also allowing for power scaling. The advantages of the picogrid can thus be summarised as follows;

- The system can automatically increase its power capacity by allowing a mixture of different sources (hybrid) to be easily added to the system in order to increase its capacity.
- The power capacity can range between 15-200 Watts depending on the minimum power of one source or storage node as well as the number of sources or storage nodes added.
- Any node can be easily added to the Picogrid in a “*plug and play*” manner without requesting for any user input command.
- The system has self-recovery properties when it comes to recovering from faults such as open and short circuits. This happens without any requests from the user.

- Additional storage nodes can be connected to the picogrid in order to provide more backup power storage at night. Each storage node can also have a different battery type from the other storage node (e.g Lithium ion and lead acid battery)
- Loads can be added at any point on grid through each node's three point connection thereby giving the user the flexibility of powering up different rooms in a house.
- The system employs a decentralized control strategy as opposed to centralized control. This ensures that the system still operates even if one node malfunctions as opposed to stopping the whole system from operating if the master controller malfunctions.

This research will thus be demonstrating the above advantages by looking at the hardware and software requirements for the system to function as required. Currently existing LVDC systems like solar home systems and pico-systems, discussed in the following chapter, were introduced much earlier into the rural market but because they are not scalable, they become unsuitable for off-grid rural electrification. The problem arises from the fact that they are manufactured as a single package with fixed sources and storage components and hence they can only cater for a limited number of loads [3-4].

1.2. Research Methodology

Having defined the problem of rural electrification requiring a scalable DC picogrid, the primary focus of the research is to ensure that the Picogrid concept meets the requirements for it to be applied to the physical system for deployment to rural areas.

Figure 5 shows a flowchart of the methodology process for the research. The first approach would thus involve a detailed literature review of the existing systems which try to address the problem with the aim of identifying the limitations provided by these systems as well as assisting in defining the research question. The next step will then look at the hardware and software requirements of each prototype node to be constructed. The picogrid concept will then be defined based from the requirements. Each node will then be constructed and tested individually before an overall test on the system is performed. The outcomes from the tests will then be used to evaluate whether the concept can be applied to a physical system for deployment to rural areas.

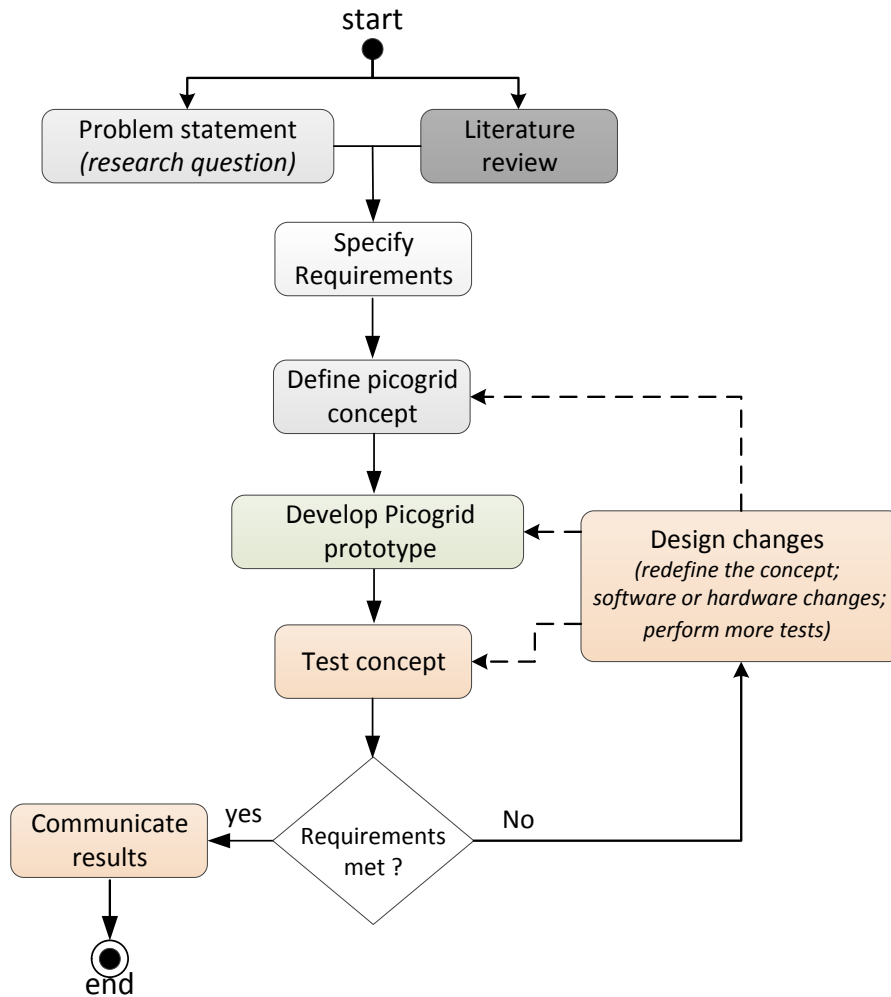


Figure 2: Research methodology flowchart

1.3. Problem Statement

This research was driven by the problem arising from the lack of electricity grid network to support the rural majority. Different solutions have been proposed over time and implemented in order to mitigate the problem of rural electrification but with less impact as the population without electricity keeps increasing in rural areas. Low power off-grid systems have been introduced in rural areas with the primary focus on providing cheap systems that can be manufactured in large quantities with ease. However, these systems are not scalable and therefore end up being limited to supplying one or limited number of loads.

1.4. Research Question

Figure 5 clearly shows how the following research question was formulated from a thorough literature review;

Question: How can the protection and control schemes of a scalable hybrid DC Picogrid be improved based on a grid code concept?

In order to answer the question, the following different sub-questions need to be answered;

Sub-Questions: 1. What different protection schemes are available for the Picogrid? (both hardware and software)

2. How is scalability achieved on the Picogrid?

3. What defines a grid code concept?

4. Can the Picogrid's stability and scalability be improved by protection?

5. Can the grid code perform well with protection?

6. Is the grid code suitable for LVDC systems?

1.5. Scope and Limitations

The scope of this research is limited to improving the concept of the picogrid and applying it to a prototype for testing purposes. This research is not focusing on the cost of materials used as most of the parts used for the prototype have been made available by the school. Hardware design issues like robustness, protective material used and rigidness of the system are also beyond the scope of the research.

1.6. Report Outline

This dissertation is structured as follows;

The first chapter is introduction. This chapter has provided clear background information leading to the conduction of the research by defining the problem at hand as well as providing the research methodology and scope.

The second chapter gives a background study on the global access to energy with specific emphasis on sub-Saharan Africa.

Chapter three provides a literature review of the techniques and methodologies used by existing LVDC systems and summarises their limitations.

Chapter four follows with the Picogrid concept and operation. This chapter provides detailed information on the operation of the picogrid by looking at the grid code command for each node and how protection and power scaling of the system are achieved.

Chapter five is Picogrid Implementation. This will discuss the construction of four prototype nodes in the laboratory for testing the Picogrid concept. The structure of each node is presented in terms of the hardware and software features.

Chapter six introduces the control system and protection schemes implemented on the system. Each node's control software implementation and protection is discussed in detail.

Chapter seven presents the tests and results performed on each node and the overall system. All findings related to the testing of the concept are detailed in this chapter.

Chapter eight concludes with future recommendations based on the test outcomes from the previous section.

2. Background

This chapter looks at the global access to energy, focusing mostly on sub-Saharan Africa that is in need of LVDC systems due to the lack of electricity

2.1. Global Access to Energy

In order to understand the rural electrification problem, it is important to look at the distribution of energy around the globe. According to a report by the World Energy Outlook 2014 (WEO) [5] and the World Energy Outlook 2016 Electricity Access Database (EAD) [6], the world currently has approximately three billion people relying on traditional biomass for heating and cooking and has about 1.5 billion people, which account for about 22% of the world population without access to electricity and clean water [7-13]. The projections made by the International Energy agency [6] on the 48% significant growth in the world energy demand in a 28 year period (from 2012-2040) could mean a further increased shortage of energy if more investments are not geared towards renewable energy.

2.2. Access to Energy in Africa

Sub-Saharan Africa and India combined constitute just over 73% of the 1.5 billion people worldwide without access to electricity, with sub-Saharan Africa dominating at about 630 million people [9]. It is the only region in the world where the number of people living without electricity is increasing as rapid population growth is outpacing the efforts made in order to provide energy access [9]. The main reason for this can be attributed to the lack of initiatives by the national utility grid to build long expensive power lines to the rural communities as they contribute less to the market. However, the continent has rich energy resources sufficient enough to meet the domestic needs of its population but fails to do so because of the political instabilities affecting most countries as well as poverty. As a result these resources are not evenly distributed within the continent [7], [9].

On average, sub-Saharan Africa still dominates in terms of having the lowest rate of per capita energy consumption of any major world region by having remained unchanged at close to 400 kWh/capita for the last decade [9]. This is less than the electricity needed to power one 50 Watt bulb continuously for a year. Figure 2 shows the Living Scale Mechanism (LSM)

triangles adopted from the WEO 2016 - Electricity Access Database [7] comparing the energy consumption between rural and urban sub-Saharan Africa.

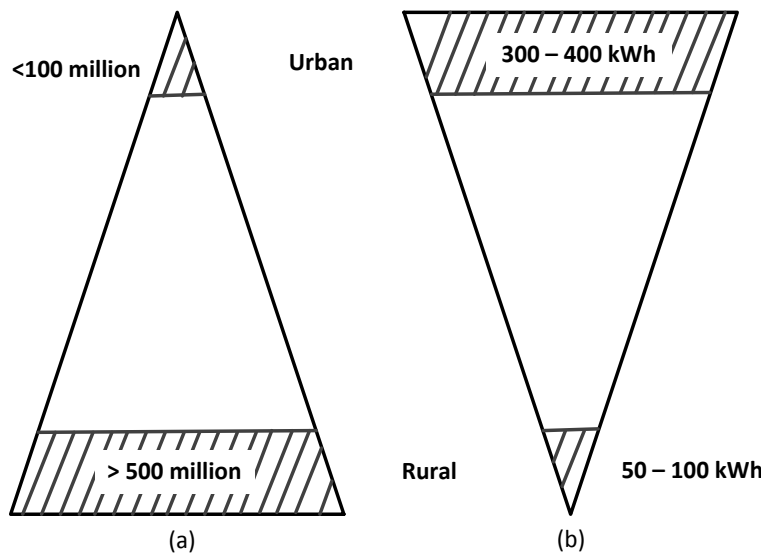


Figure 3: The LSM triangles of sub-Saharan Africa population showing; (a) Urban and Rural Population versus (b) Energy consumption per capita

From figure 2, the urban residents get the benefit of large power consumption from the utility as they can afford the electricity, whereas the poor majority get little or no power supplied to them mainly because of the high costs incurred in transmitting electricity to the rural areas.

2.3. Africa's Energy Consumption per Capita versus Carbon Dioxide Emissions

Modern society is totally dependent upon energy in the form of electricity derived from burning fossil fuels. Petroleum, natural gas and coal still remain the highest sources of energy used globally as shown in figure 3. The burning of these fossil fuels releases carbon dioxide into the atmosphere, thereby increasing the greenhouse effect.

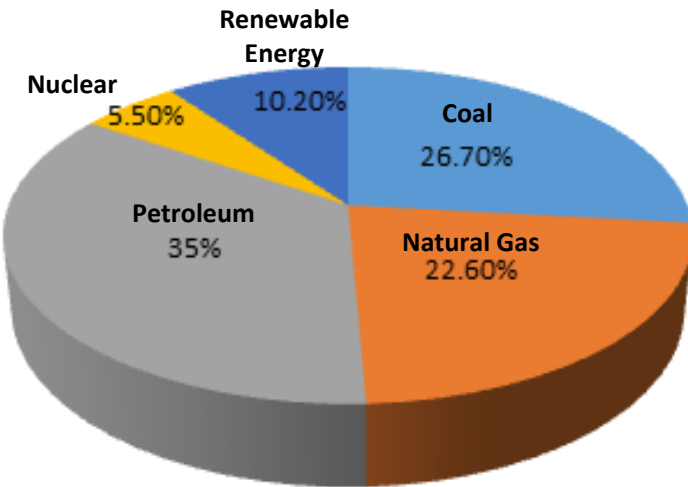


Figure 4: Global energy consumption by source [6]

The energy consumption per capita refers to the energy consumption per person in a particular country [9], measured in kWh/person. Most developed countries such as the UK and Canada have a high kWh/p whereas the majority of developing countries found in sub-Saharan Africa have a low kWh/p [9], [13]. This is a clear measure of the lack of access to electricity in the rural areas of sub-Saharan Africa.

The growing global demand for energy consumption per person (capita), whilst limiting the amount of carbon dioxide emitted to the atmosphere is what needs to be adopted by developing countries of sub-Saharan Africa. Off grid renewable energy resources of LVDC nature and not in the form of Independent Power Producing Plants (IPPPs) offer the solution for rural electrification whilst limiting Carbon Dioxide emissions. Renewable energy IPPs offer rather clean energy that is mainly fed back to the utility grid so as to increase the capacity. However, the same power only caters for the small urban population who can afford the electricity.

Countries such as Canada, Australia and UK have adopted the Kyoto Protocol [14] which aims at reducing the global greenhouse emissions by encouraging countries to introduce more renewable energy solutions. As depicted from figure 4 below, developed countries have little carbon dioxide emissions compared to developing countries across the globe. This can be attributed to the fact that most developed countries are relying more on the renewable energy sources with time. The introduction of this protocol together with other green initiatives in European countries has boosted the energy consumption per person whilst limiting the carbon dioxide emissions.

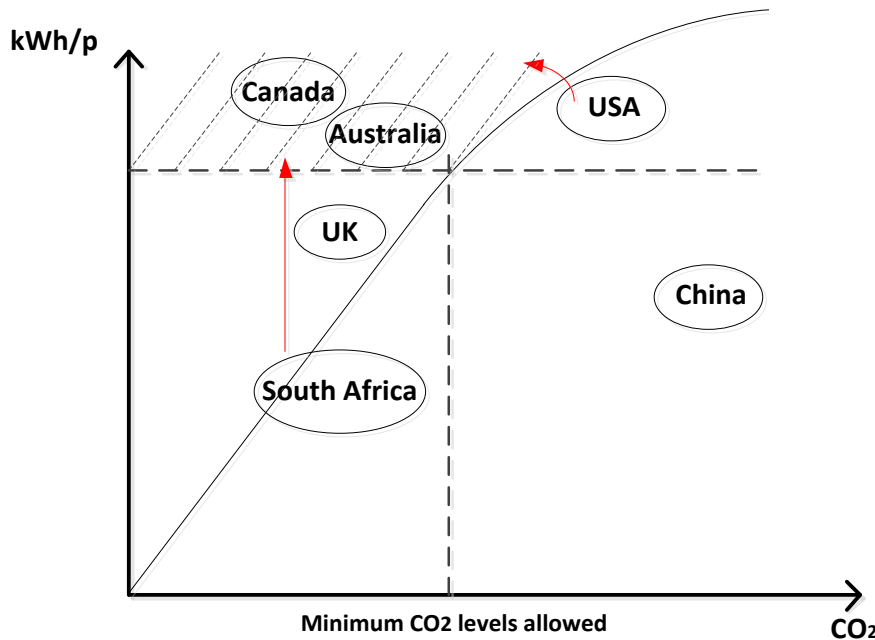


Figure 5: Global Carbon Dioxide emissions vs Energy per Capita (kWh/Person)

From figure 4, the Kyoto Protocol encourages every country to move towards the shaded region by encouraging the use of renewable energy. Countries like USA only need to include more renewable energies of any form in order to reduce the Carbon Dioxide emissions as the country's energy consumption per capita is high. However, Sub-Saharan African countries need to increase both kWh/p whilst also reducing Carbon Dioxide emissions in order to achieve the target. The introduction of multiple off-grid renewable LVDC to rural sub-Saharan communities would thus allow developing countries like South Africa to move to the target zone as shown by the red arrow.

2.4. Summary

This chapter has looked at the electrification rate of sub Saharan Africa by comparing the energy consumption per capita in rural areas to urban areas. It was found that the majority of urban residents enjoy surplus energy as indicated by high levels of energy per capita. The majority of sub Saharan Africa population lives in rural households with little or no access to electricity as indicated by low levels of energy per capita. The next chapter will propose LVDC systems as possible solutions to electricity access for the sub Saharan Africa rural majority.

3. LVDC Systems for Rural Areas

3.1. Introduction

This chapter introduces currently existing LVDC systems for rural application. A discussion on how these systems have penetrated the rural market but still not reliable in some areas will be presented. An introductory brief on the control algorithms used by these systems is also provided.

Extensive research is being done into LVDC systems worldwide [15] as the current technology focuses mainly on reducing costs and not scalability. Scalability refers to the increase or decrease in the size of a system in terms of its power output so as to meet the load demand. The International Energy Agency report on PV systems [16] discusses a few of the existing renewable energy solutions offering LVDC systems to rural areas but are not scalable as they are manufactured with fixed sources and storage components.

3.2. Single-Source, Single-Storage and Single-Load systems

Solar lanterns or solar lights such as shown in figure 6 fall under single source, single storage and single load LVDC systems. These systems were introduced as replacement for kerosene lamps used mostly in eastern and western sub-Saharan African countries [17-18]. Each solar light comes with a single source, storage and light thereby making it cheaper and easy to use. However, it becomes unreliable when more power capacity is demanded from the system as one would need to purchase a number of these lights for each room in the house due to the fixed nature of sources and storage components. The battery always requires replacement after some time and hence it would be hard to access without having to completely dismantle the entire system.

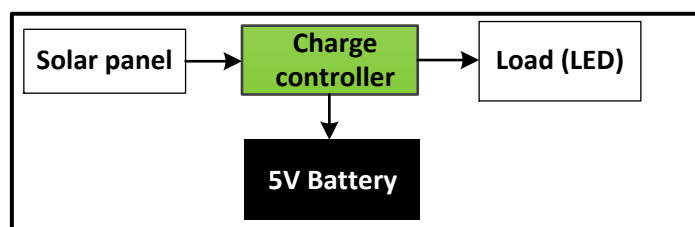


Figure 6: Solar light structure

3.3. Single-Source, Single-Storage, Multiple-Load Systems

Solar Home Systems or Pico PV Systems (PPS) are examples of single source, single storage and multiple load systems which come in different sizes depending on the user requirements. These systems were introduced in order to tackle the problem of single loads by providing an option of adding more loads to one system. There are SHS for both rural and urban homes which differ in power capacity [18]. SHS systems with more than 100W power output are normally offered to users on a pre-paid basis as most of them cannot afford to buy them in cash. In rural areas, SHSs are mostly used for lighting as well as powering small scale household electronics such as radios [19]. The systems have also improved rural standards of living for most women and children requiring light for cooking and studying purposes [20]. As shown in figure 7 and in the IEA report on PV systems [21], a SHS offers more flexibility by having limited number of ports for connecting small loads such as LEDs and cell phones. However, the system is also manufactured as a complete package with a permanent source and a battery. This makes it unreliable and expensive. Also, the size of the battery and solar panel are designed to meet a limited number of loads.

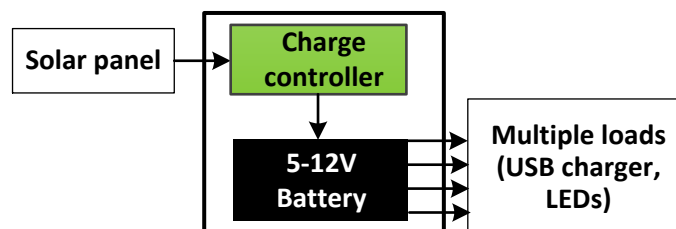


Figure 7: A Solar Home System structure with multiple nodes

Another example of a SHS designed for rural application is the Schneider SHS [22] which isolates the battery from the solar light as shown in figure 8. Users are allowed to purchase only the lamp and the battery is rented to them on a daily basis. Although this relieves the user from battery maintenance issues, the need for more solar lights would mean spending extra money on buying and charging the units. The system also offers a separate charging station for up to ten Schneider batteries but this station relies on the mains electricity in order to charge the batteries. Also system maintenance is managed by the manufacturers as opposed to local community members.

As tabulated in table 1, there are other types of SHSs on the rural market providing different features for enhanced power outputs. However, most of these systems offer limited power

scaling capabilities mostly to keep the cost of the system low. Table 1 summarises some of these LVDC SHS currently deployed in sub-Saharan Africa.

Table 1: Summary of the location and power capacity of different SHS in sub-Saharan Africa

SHS	Location	Power range (W)	Appliances Powered
Schneider SHS	Africa, India	10-1000	LEDs, Cellphone, Radio, DC TV, DC refrigerator
Mobisol	Tanzania, Rwanda [33]	30-200	LEDs, Cellphone, Radio, DC TV
Solar Now SHS	Uganda [23]	50, 500	LEDs, Cellphone, Radio, DC TV
Ready Pay SHS	Uganda [32]	10-34	LEDs, Cellphone, Radio
iShack SHS	South Africa [30-31]	< 100	LEDs, Cellphone, Radio, DC TV
Phaesun	Somalia [33]	<200	DC refrigerator

Prepaid solar home systems such as the iShack [31] are penetrating the rural market due to the pay-per-use services that makes the systems cheaper as well as having crucial loads such as DC TVs as a package. However, the systems are still not scalable as scaling up would require a completely new system for each extra load.

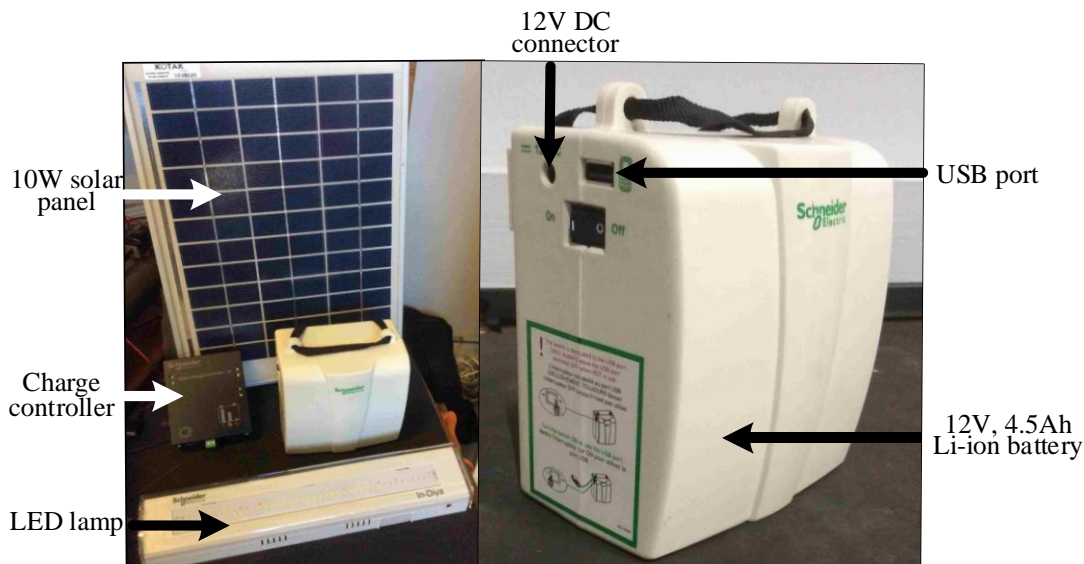


Figure 8: Schneider Solar Home System

3.4. Single-Source, Multiple-Storage, Multiple-Load Systems

An example of multi-storage, multi-load system is a Pico lamp. The lamp has local storage and charge controllers for its LED load. This has been found to increase the systems efficiency [24] when compared to a SHS with one storage for all loads. However, unlike a

solar light, a Pico lamp offers additional features which make it partially scalable. Up to four Pico lamps can be connected together to form a small grid that makes power sharing possible. Figure 9 presents a structural diagram of two pico lamps. The system also provides extra USB ports for charging cellphones but cannot be scaled up further than four Pico lamps and only allows for one solar panel input. Also due to the lack of an isolated battery node, one would need multiple pico lamps in order to increase the system's capacity instead of just having to add more batteries. Problems would also be encountered during maintenance as the whole lamp has to be dismantled in order to replace the Lithium Ion battery when its lifespan has been reached.

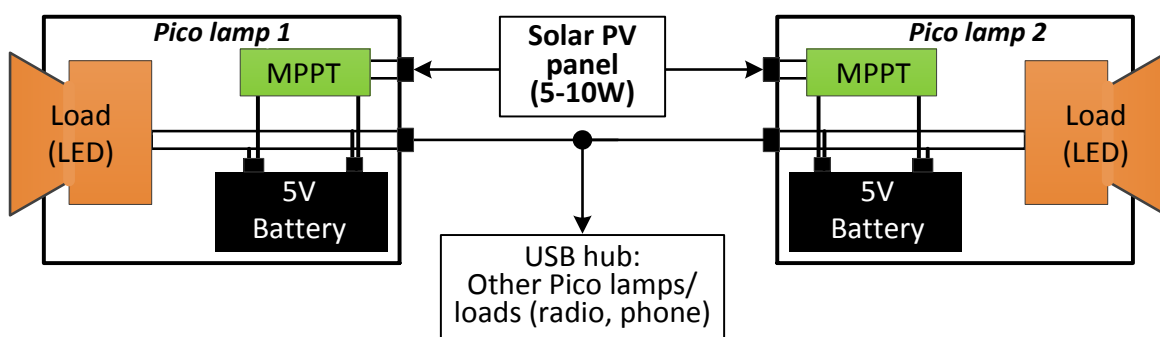


Figure 9: Two Pico lamps connected together for power sharing

3.5. Multiple-Source, Multiple-Load and Single-Storage Systems

An example of a system with multiple sources, multiple loads and single storage components is the Renewable Energy Hybrid System (REHS) shown in figure 10 developed by Sharetech [26]. The system consists of solar, wind and a human pedalling generator as its sources. Each module is able to operate independently or as part of the hybrid system through a centralized controller. A REHS DC Bus can be scaled up to 50V. However, the system's reliability is questionable as all controllers are located inside and linked together by a central controller. This means that the entire system malfunctions if the main controller malfunctions. The system's DC-AC inverter not only produces power losses but also becomes costly as it needs special controllers for making it compatible with 230 V AC loads.

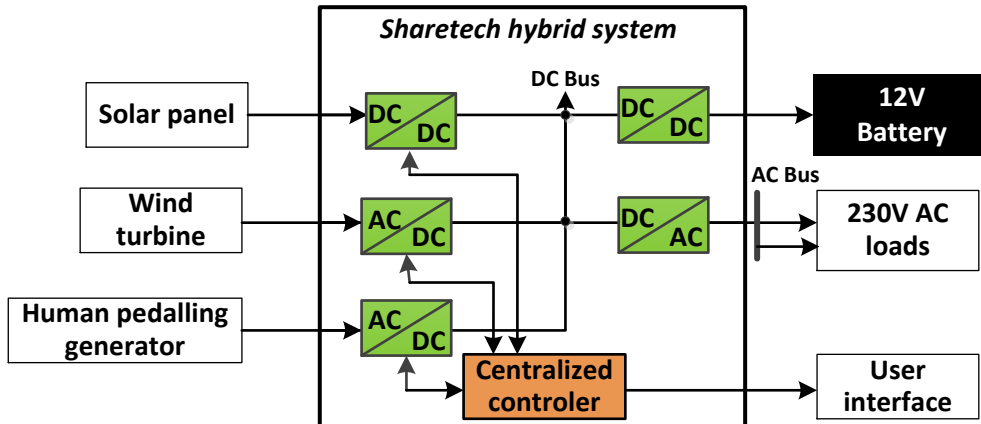


Figure 10: Sharetech hybrid system structure [26]

3.6. Pre-Paid Solar Home Systems

Pre-paid Solar Home Systems are offering an upcoming market in Africa whereby residents are supplied with SHSs at no upfront costs and made to pay for them over time through prepaid services. These systems are popular in remote areas of sub-Saharan African countries such as South Africa [27], Tanzania [30] and Uganda [21, 23]. Although cheap, the system is not scalable as its power is limited to a particular number of loads. More load demands would thus require scaling up to a completely new system.

3.7. Stand-Alone DC Microgrids

Stand-alone DC Microgrids do not fall under LVDC systems due to the high DC voltages and power they generate. However, DC Microgrids such as the one shown in figure 11 offer an alternative solution for rural community or villages as opposed to single households [27-29]. This is because microgrids are too expensive to put in place and maintain due to the large power generation that needs synchronisation with the utility grid and power factor correction. This makes them too complex to be handled by rural communities for maintenance purposes. As shown in figure 11, a DC microgrid has a complex Point of Common Connection (PCC) linking the utility grid to the customer's loads. This requires constant monitoring and as a result becomes too expensive as trained personnel is required to analyse and maintain the system.

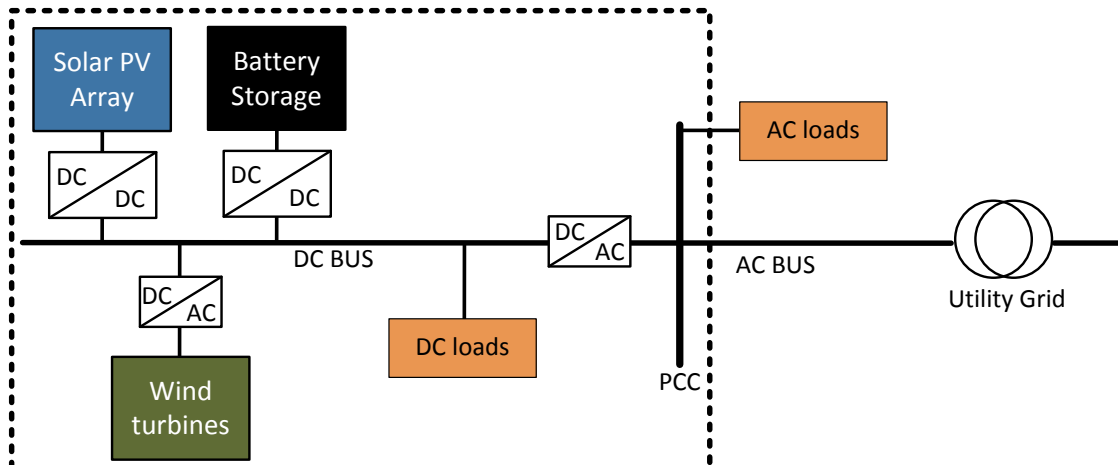


Figure 11: A Stand Alone DC Microgrid structure

3.8. Droop Control of LVDC systems

Except for DC microgrids, the LVDC systems described above have centralised control schemes which only respond to changes in the system's bus voltage levels. These systems offer limited control of the load current by having a fixed current limit defined by the maximum power output of the system. This is what makes them not scalable.

The proposed Picogrid has both voltage and current control schemes, thereby making it similar to the droop control of voltage and frequency in stand-alone DC Microgrids [34-36, 50-52]. By having more sources and storage nodes, the overall load current limit increases and in turn increasing the power output of the system. The maximum power limit will be determined once the cable design process has reached.

3.9. Summary

This chapter has looked at the existing LVDC system currently deployed in rural sub-Saharan Africa. A common limitation of all the systems is the lack of power scaling due to centralised controllers with fixed load current thresholds.

Single-source, single-storage and single-load systems like the solar lanterns and solar LED light were found to have fixed power outputs made possible by centralised controllers. This centralised control together with packaging of all components in one package limits the power output to an extent of having to purchase a completely new system in order to have more light intensity in a room.

Single-source, single-storage and multiple-load systems like the SHSs and Pico lamps have been found to be increasingly popular than solar lanterns because of the extra loads they offer. However, they also have centralised control systems which hinders them from being fully scalable. This also applies for multiple sources, multiple storage and multiple loads LVDC systems. Although they use a mixture of different sources in order to supply a number of loads, having a centralised control system limits power scalability.

Stand-alone DC Microgrids have decentralised controllers but do not belong in the LVDC category. DC Microgrids allow for scalability through droop control of frequency and voltage; a similar strategy that was proposed for the picogrid but current was controlled instead of frequency.

The next chapter looks at the composition of the Picogrid by providing its structure and operation on how power scaling is achieved through multiple sources, multiple storage and multiple loads.

4. Picogrid Structure and Operation

4.1. Introduction

The previous chapter has highlighted the main problem with currently existing LVDC of not being power scalable. This chapter introduces the structural blocks making up the proposed Picogrid together with its operation which makes power scaling possible. A set of rules defining the state of the Picogrid Bus Voltage (PBV) for each node is also presented. These commands, best described as the “*Grid Code*” ensure that the stability of the Picogrid is maintained and faults are eliminated before causing damage.

4.2. Picogrid Structure

As seen in figure 12, each node comes with its own controller and three port connections for simplifying the power scaling process. The user simply “plugs and plays” different nodes together in order to meet load requirements. The components making up each node can thus be summarised in Table 2 below;

Table 2: Node structural components

Node	Component				
	Flyback converter	controller	24V Power supply	24V – 12V DC – DC	PBV indicator LEDs
Solar	√	√	√	√	√
Wind	√	√	√	√	√
Storage	√	√	√	√	√
Load	X	√	√	X	√

From Table 2, each node is autonomous with its own controller, a 24V supply and PBV indicator LEDs showing the different PBV seen by each node. The details of each component are discussed in chapter 5 which deals with implementing the grid code to a prototype.

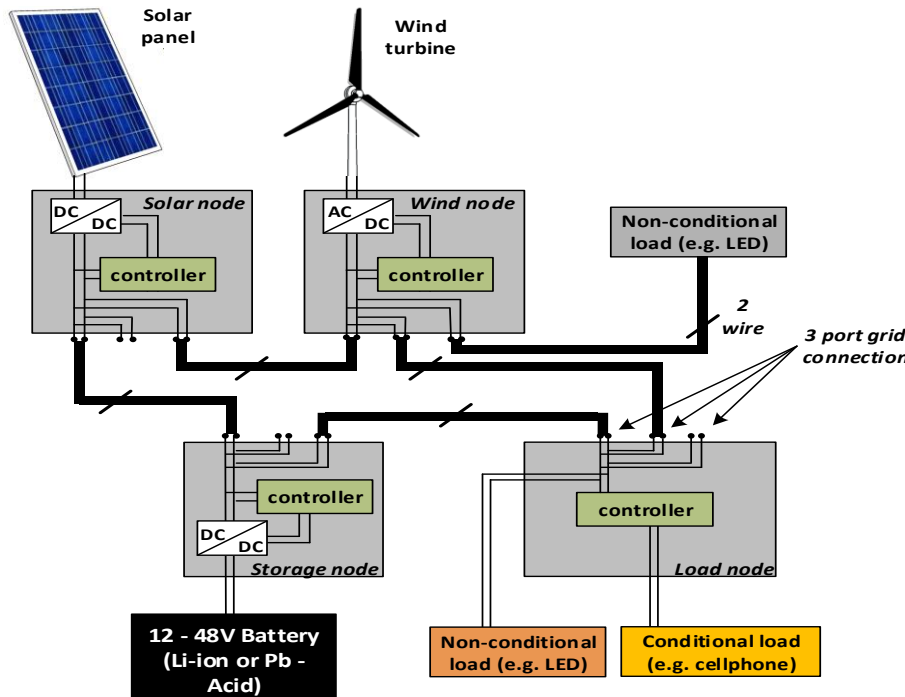


Figure 12: Hybrid DC Picogrid

4.3. Picogrid Operation

4.3.1. Grid Code

A Grid Code defines the set of rules that must be obeyed by every node on the picogrid in order to achieve stability and allow for scalability. As shown later in figure 14, these rules are determined by the state of the PBV. Each node has its own PBV indicator LEDs for communicating to the end user the current state of the picogrid. The PBV was derived from typical lead acid charging and discharging voltage.

Stable State ($V_{nominal}$): As shown in figure 13, the green region represents the stable state. This is the ideal state of the grid at 12V with a $\pm 1V$ range for stable operation. The choice of this voltage arose from the easy availability of existing 12V car batteries. Not only are they cheap, but they are also easily accessible [37-38]. Each node performs the following autonomous task;

- A source node either decreases or increases its production depending on whether PBV lies above or below 12V.
- A storage node will initiate the charging process when the PBV lies between 12V-13V so as to maintain the PBV within the stable range by absorbing the excess power.

When the PBV is between 11V and 12V, a storage node initiates the power discharging process so as to maintain stability.

High Voltage State (V_{high}): This state is shown by the upper orange region in figure 13. This is most likely to occur when there is excess power from the source nodes due to strong winds or sunshine leading to the bus voltage rising above the stable operating point (i.e 13V-14V). This can also occur when small power consuming loads are connected to the grid. The Picogrid is then pushed into the high voltage state leading to the following actions;

- The storage node increases its charging process provided the state of battery charge is less than 100%. At 100% the supply of current is cut.
- High voltage amber LEDs are activated in order to alert the user to connect more loads if available. If the user is not around then the voltage ultimately goes into over voltage mode.

Over Voltage State (V_{over}): This is shown by the upper red zone in figure 13. In this state, the supplied power has exceeded the power demand from the end users by a large margin such that the bus voltage rises above 14V. This can also occur when a storage node's battery is fully charged. The node trips and restarts after a time delay. A red PBV LED is activated on all nodes in order to indicate the state of the picogrid.

Node Status				
Picogrid Bus Voltage	Grid Status	Source node(s)	Storage node(s)	Load node(s)
20 V	V over	Trip, sleep & restart	Trip, sleep & restart if battery is full	Trip, sleep & restart
14 V	V high	Decrease Production	Increase charging	Increase load
13 V	V nominal	Decrease Production Increase production	Initiate charging Initiate discharging	Increase load load shedding 1
11 V	V low	Increase production	Increase discharging	load shedding 2
10 V	Vunder	Trip,sleep & restart	Trip,sleep & restart	Trip,sleep & restart
0 V				

Figure 13: Picogrid Bus Voltage (PBV) code

Low Voltage State(V_{low}): This is shown by the lower orange zone in figure 13. This state occurs when heavy loads are connected to the grid such that the available sources cannot support them. This can also occur when there is not enough power from the sources due to cloudy or less windy days. This ultimately leads to the bus voltage dropping into low voltage mode (i.e. 10V-11V) with the following actions occurring;

- A storage node initiates the discharging process provided that the batteries are not empty. The power from the batteries is then used to support the grid and in turn stabilize the system. If the batteries are empty the picogrid is pushed in-to under voltage mode. The absence of a storage node would eventually push the picogrid into under voltage state.
- A load node will initiate the first load shedding phase on conditional loads such as cellphone chargers or any other appliances with battery backups when the PBV is between 10.5V – 10.9V. Conditional loads are the non-essential loads such as cellphone and laptop chargers which are not connected for a long time on the grid. Non-conditional loads such as lights and refrigeration are essential as they are operated constantly for a long period.
- All load nodes will initiate the second stage of load shedding when the voltage drops even further than 10.5V so as to relieve stress on the grid.

Under Voltage State (V_{under}): This state, shown by the bottom red region in figure 13, occurs when there is a high power demand from the loads than the picogrid can supply. This results in the bus voltage dropping below 10V. This can also occur when the batteries are empty and hence a storage node cannot support the grid anymore. In this state, all active nodes shut down and only restart after random delays so as to allow for system recovery. A red PBV LED is activated on all nodes in order to indicate this state of the picogrid.

4.3.2. Picogrid Bus Voltage

As previously mentioned in chapter 3 section 3.8, a picogrid utilizes a form of droop control also referred to as DC-Bus Signaling (DBS) [34-36]. As shown in figure 14, this control algorithm, described in detail in chapter 6 allows each node to make its decisions based on the DC Bus voltage levels. Any node connected to the Picogrid first checks the current state of the Picogrid Bus Voltage (PBV) and then responds accordingly as shown. A PBV is defined by five different bus voltage levels; V_{under} , V_{low} , $V_{nominal}$, V_{high} , V_{over} . These voltage

levels define the grid code so as to ensure that a stable operation is achieved in the decentralized control system. Each node's control action thus relies on the state of the PBV in order to perform its required action. The control of the bus voltage and load current limiting detailed in chapter 5 and chapter 6 is what makes a picogrid's control scheme similar to the droop control of frequency and voltage in AC systems.

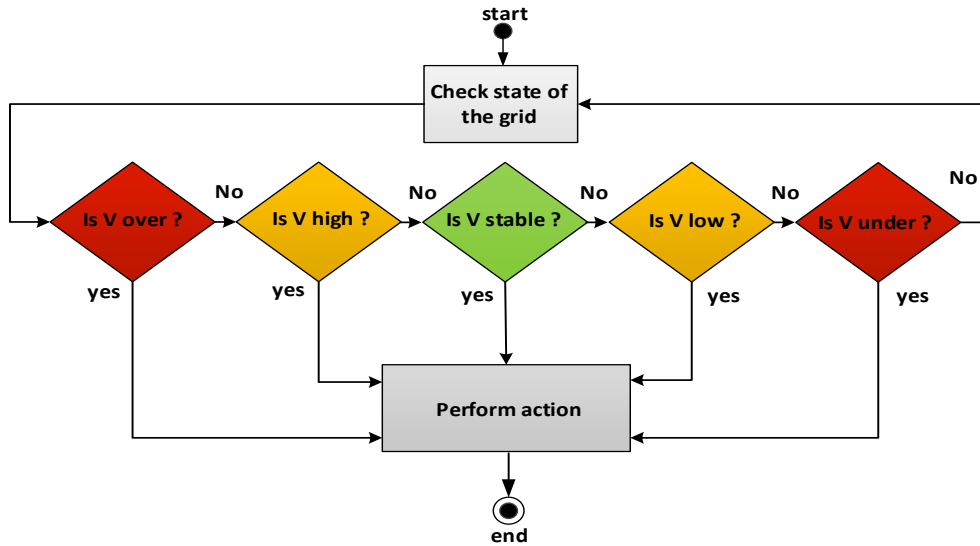


Figure 14: Node operation flow chart

Each node automatically initialises itself once its controller is powered. Details on how the initialisation process occurs is provided in the node user manual in Appendix F page 1.

4.3.3. Scalability

The power output of a Picogrid can be scaled up or down in order to meet the growing load requirements of a rural household through the addition of more sources and/or storage nodes. This is achieved in a simple “plug and play” manner connection of more sources to the picogrid. It is shown in chapter 7 that by adding more sources, the combined output current increases whereas the bus voltage remains the same. Each source and storage node has its own maximum power production determined by the electronic components and the load current discussed in chapter 5.

4.3.4. Stability

Stability on the Picogrid is autonomous and can be achieved by load shedding, addition of more loads or by storage node charging or discharging processes. Also, for demonstration

purposes, each source node has the ability to adjust the bus voltage state in order to observe the system performance in each state.

4.3.5. Protection

Protection forms the core of this research as the system is required to self-recovery from all electrical faults without requiring any form of user input. It is discussed later in detail how each node is able to self-recover from any sudden open or short circuit on the grid and automatically returns to stable operation.

4.4. Summary

The principle of operation of a picogrid has been presented in this chapter. A “grid code” defining the commands for each node on the grid has been explained with emphasis on each node’s tasks. The next chapter looks at the physical implementation of the laboratory prototype by breaking down each node into its hardware and software composition.

5. Picogrid Implementation

5.1. Introduction

The previous chapter has provided a detailed explanation on the picogrid concept which is centred on a set of rules defined by a grid code. This chapter looks at the hardware implementation of each of the four demonstration nodes to be used for testing the Picogrid concept. Each node's structure is broken down into sub-components with details on how power and information flows.

5.2. Node Structure

As shown previously in table 2 of section 4.2, each node except for a load node has a flyback converter, a controller and a 24V supply as the main components. Each node uses a 24V DC supply that is powered from the mains electricity. This was done because the controllers used for each demonstration node require 24V DC power supplies. Therefore, the nodes would most likely be placed indoors and thus would require mains supply and not from solar panels and wind turbines.

In the future when the picogrid is to be deployed to rural areas then the source nodes will obtain power from solar panels and wind turbines whereas load nodes would be powered straight from the grid. The four nodes discussed here are for demonstrating the picogrid concept and would therefore require indoor operations.

5.2.1. Source Nodes

Figure 15 shows a photograph of a solar node. The structural block diagram showing the power and information flow between components is shown in figure 16. A complete circuit diagram can be viewed in Appendix H page 1. The only difference between the structure of a solar and a wind node is that a solar node has a dimmable light for replicating solar PV energy in different weather conditions. The dimmer the light, the lower PV energy obtained. A wind node on the other hand has a motor that rotates blades like a wind turbine. The regulator knobs shown in figure 15 and figure 16 are responsible for dimming the light and regulating the motor speed so as to simulate the two conditions.

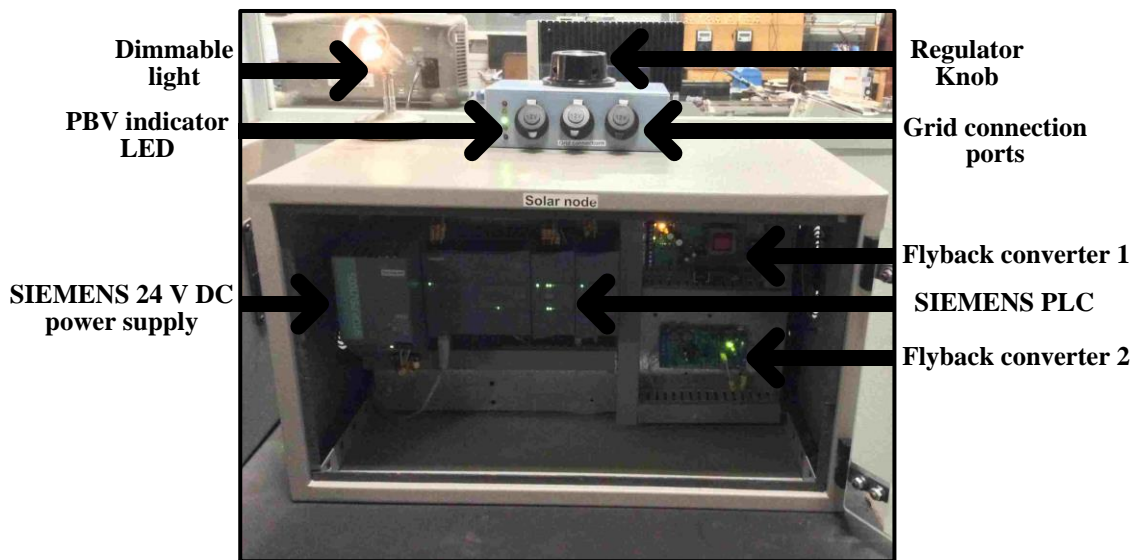


Figure 15: Solar node photograph

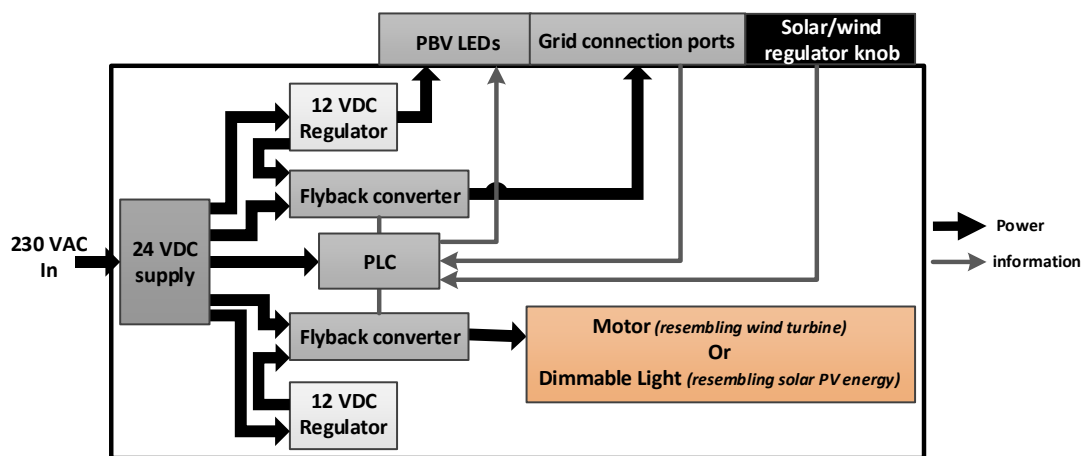


Figure 16: Power and information flow between components of source nodes (solar and wind)

From figure 16, source nodes have two flyback converters; one dedicated for sourcing the required bus voltage and the other for powering the dimmable light on the solar node or the motor on the wind node. Power from the flyback converters is made available to other nodes via the three-port grid connection points. Each source node has two 12V DC regulators that power the low voltage side of the flyback converter as well as the PBV LEDs. The solar/wind regulator knobs send information to the PLC which then sends information to the flyback converter to control the light or motor.

5.2.2.Storage Node

Figure 17 and figure 18 show a storage node having one flyback converter instead of two. A complete circuit diagram of a storage node is presented in Appendix I page 1. Ideally it should have two flyback converters with one for sourcing and the other for sinking current depending on the state of the bus voltage. However, since a storage node has no real life battery, a choice was made to use the HMI display to show the battery properties and hence act as the virtual battery for the system. Also, only sourcing converters were designed for this research. From figure 18, a controller (PLC) constantly monitors the grid voltage and switches between sourcing or sinking current depending on the state of the bus voltage. Each state is captured and displayed on the HMI screen.



Figure 17: Storage node photograph

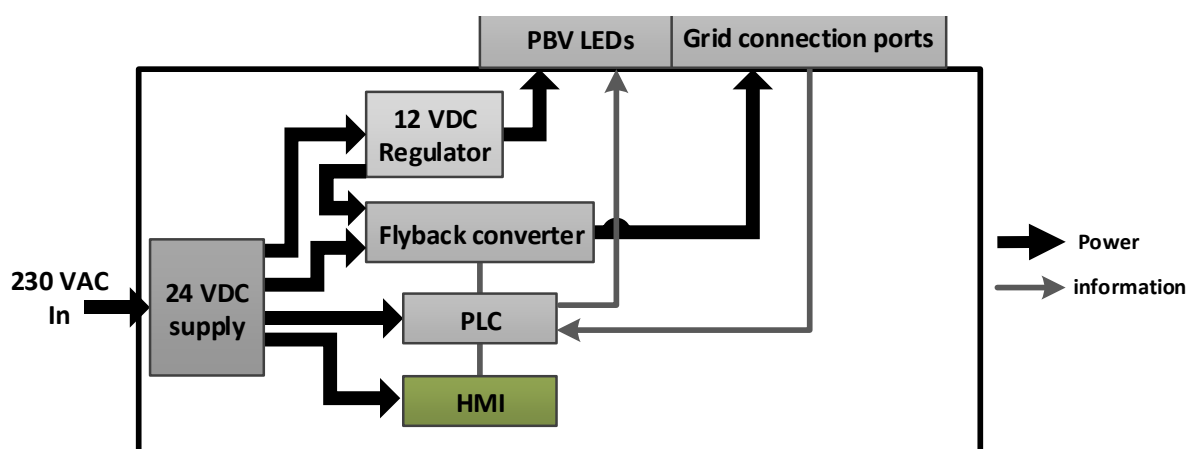


Figure 18: Power and information flow between components of a storage node

Each component shown in figure 18 is discussed in detail in section 5.3.

5.2.3. Load Node

Figure 19 shows a photograph of a load node with conditional and non-conditional loads located on the left and right respectively. Figure 20 shows the power and information flow block diagram of the load node demonstrator circuit diagram presented in Appendix G page 1. The 24 V supply powers both the PLC and the PBV LEDs. Conditional and non-conditional loads are powered by a storage or a source node connected to the grid ports. Conditional loads are also connected to the grid connection ports via a manual switch so as to draw power from the grid. A PLC performs load shedding depending on the state of the PBV. Details on load shedding control aspects are discussed in chapter 6.



Figure 19: Load node picture

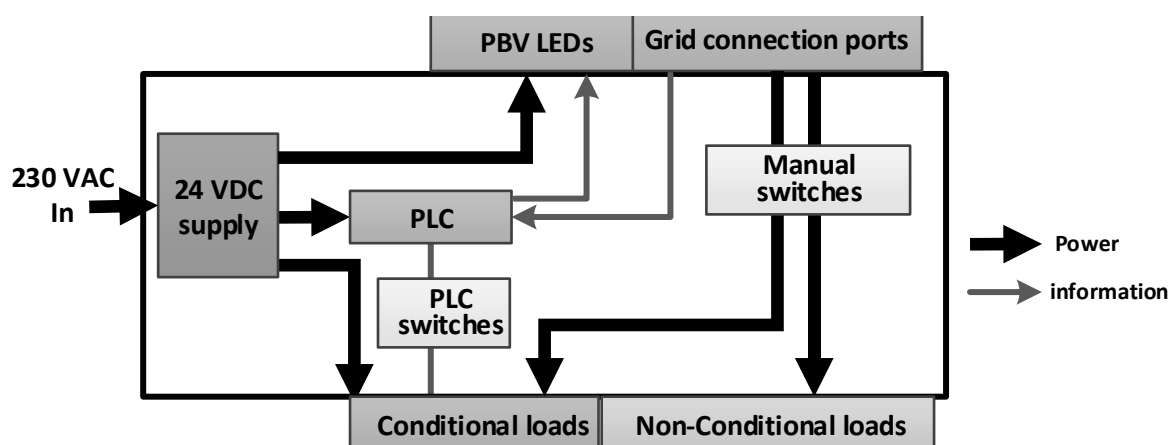


Figure 20: Load node power and information flow block diagram

5.3. Node Components

5.3.1. Flyback Converter Circuit

A flyback converter forms the core of any source or storage node. This is because it is responsible for setting the bus voltage and hence supplying power to the grid. A flyback converter was chosen not only for its simplicity and low cost but also due to the complete isolation it provides between its primary and secondary side and also being able to operate over a wide range of input voltage variation [39-41]. Also for power outputs less than 100W, the design of the inductor transformer is simple and hence cheaper [42]. This is crucial for overvoltage protection because the secondary side is where all the different voltages from other nodes meet via the grid connection ports. Thus the secondary side is what forms the picogrid as it is the point of connection to the grid. This means that any fault on the picogrid such as a short circuit will be isolated from the primary side and therefore protecting the internal circuit components. This research was limited to improving the following aspects of an existing flyback converter of a previous research project [43];

- Flexibility in terms of different flyback operation and configuration modes
- Voltage Control Mode (VCM) - For improving voltage stability in the stable operating state and also improve load variations.
- Current Control Mode (CCM) - For load over-current protection (load current limiting) as well as improving load variations.
- Opto-Isolation of the VCM loop - in order to completely isolate the primary side from the secondary side of flyback converter.

Improved Flyback Converter

It is important to mention that each source and storage node has a slightly different flyback converter as some of the improvements were applied to newer versions of the flyback PCBs when some of the nodes had already been constructed. Table 3 below summarises the flyback converter version applied to each node with the storage node having the latest version. This is reflected later in chapter 7 tests.

Table 3: Improved flyback converter versions showing major improvements for each node

Node	Flyback converter version	Major Improvements
Wind	1	Voltage Control Mode (VCM)
Solar	2	VCM
Storage	3	VCM, CCM – fastest response of all nodes

A full schematic diagram of the improved flyback converter is presented in Appendix A page 2. Details on the design, operation and the different configuration modes that allow the flyback converter to operate at maximum duty cycle (equating to maximum power) are presented in Appendix B page 1.

Voltage Control Mode (VCM) and Current Control Mode (CCM) regions

As shown in figure 21, the flyback converter was divided into two sub-components; VCM and CCM regions. The VCM region shown by the orange rectangle in figure 21 deals with voltage feedback from the secondary side of the converter. This loop is responsible for controlling the varying bus voltage and as a result protects the converter from over voltages caused by sudden open circuits arising from the sudden removal of load. This meant that a complete redesign of the PWM controller chip operation [45] was necessary in order to allow the converter to operate at maximum duty cycle without compromising the MOSFET and the PWM chip.

The VCM loop was also modified by including an isolation amplifier within the feedback loop for providing complete isolation between the secondary output voltage and the low voltage primary side of the PWM controller chip and hence protecting the system from over voltages. Details on the isolation amplifier design and operation are presented in Appendix D page 1 to page 5.

As seen in figure 21, VCM resistors (R1 and R2) are responsible for setting the desired reference value to feed back to the PWM chip. A controller was also used to control the voltage of source nodes by constantly monitoring the voltage and sending reference voltage to PWM comparator. The voltage divider presented by resistors R5 and R6 in figure 21 was used to drop down the bus voltage to specific analogue input limits of the controller.

As shown in figure 21 by the green shaded region, CCM deals with regulating the load current of the flyback converter and as a result protecting the PWM chip and the MOSFET from high short circuit currents [39]. By limiting the load current, the system is protected from accidental short circuits as the PWM chip automatically switches off. The current limiting resistor (R_{lim}) is responsible for limiting the load current by shutting down the PWM chip.

A complete design process for determining both VCM and CCM resistors is provided in Appendix C page 1- page 7. Table 4 below shows a technical comparison between the original and the improved flyback converter. All the components used for the flyback converter circuit are detailed in Appendix E.

Table 4: Technical specifications of old versus Improved flyback converter circuit

	Old flyback	Improved flyback	Nominal
PWM Input Voltage (V)	9-20 V	9-20 V	12 V
Switching Frequency	100 kHz	42.7 kHz	-
MOSFET drive input voltage (V)	18-32 V	18-32 V	24 V
Output Voltage (V)	12V	12V	12 V
Load Current (A)	0.24 -0.48A	0.24 -2A	11-13 V
Source/Storage node Power (W)	3.5	> 15	
Total Power of three nodes (W)	10.5	> 50	

From table 4, it can be seen that the load current range of the improved flyback converter was increased by nearly five times thereby raising a source or storage power by more than seven times at the required output voltage (12 V). The switching frequency of a flyback converter is advised to be below 100 kHz for the sake of simplifying the inductor-transformer design as well as allowing for smaller component choice which makes the overall system cheaper. However, the frequency was halved as a high switching frequency increases switching losses which were found to overheat the MOSFET circuit.

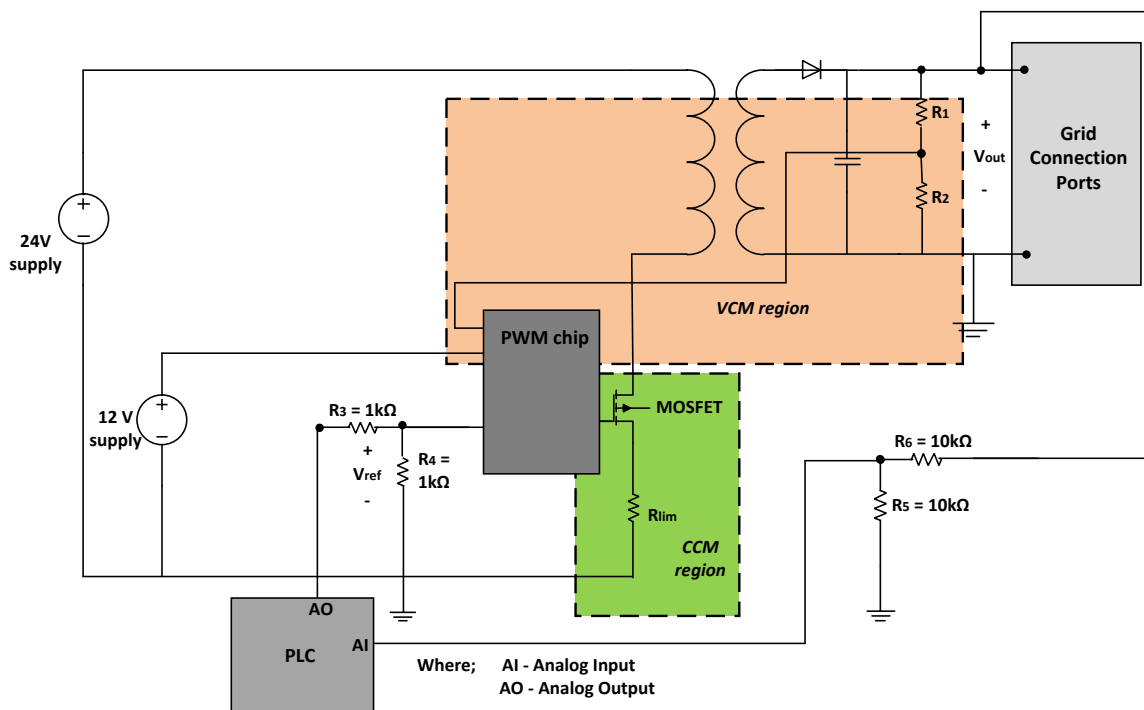


Figure 21: Flyback converter showing VCM and CCM regions

5.3.2. Controller

All demonstration nodes each use four Siemens Simatic S7 -1200 high speed PLC controllers [46] in order to achieve the required functionality. Although this controller is expensive in nature, its availability combined with high efficiency makes it ideal for the picogrid application. It has a DC supply as well as 12 relays that can be used for different control features.

As shown in figure 22, the main objective of a PLC is to constantly monitor the bus voltage and perform the following different roles;

- Provide a reference voltage to the source node's flyback converters.
- Controlling of dimmable light and motor on solar and wind nodes respectively.
- Control the switching of PBV LEDs of each node.
- Perform load shedding on conditional loads.
- Sending information on state of battery charge to the storage node HMI.

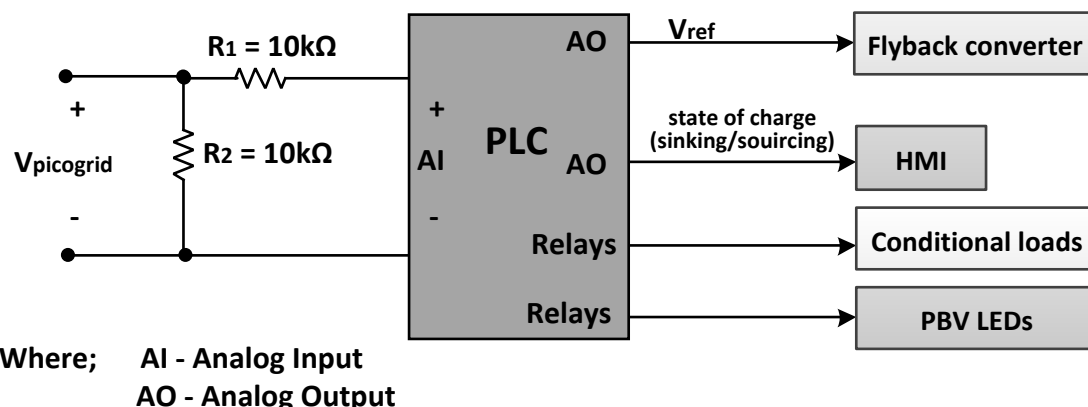


Figure 22: PLC functional block diagram

From figure 22, the voltage divider ensures that the PLC's input limits of 10V are not exceeded [47] with the change in PBV. AI and AO stand for Analog Input and Analog Output Respectively. AI converts all analog input voltage values to machine language that is processed by the controller. AO performs the reverse process. Details of the software control aspects are provided in chapter 6.

5.3.3.24 VDC Power Supply

Siemens high current output 24V power supplies were used to power each node's PLC [47] as well as the primary side of the flyback converter PCB. Each power supply is able to provide enough current needed by the node components. The supply uses 230V AC from the mains electricity and converts it to a smooth 24V DC. In the future during deployment phase of the picogrid the power supply will however be replaced by solar PV, wind turbine or battery power. The PLC user manual [46] shows the connection diagrams for powering the PLCs using the given 24 V.

5.3.4.24V-12V DC Regulators

24VDC – 12VDC regulator converter chips [48] were used to power the low voltage primary side of the flyback converter circuit as shown previously in figure 21. The 12V supply was also used to power the PBV LEDs for the nodes.

5.3.5.PBV Indicator LEDs

Picogrid Bus Voltage indicator LEDs shown on the node photographs in figure 15, figure 17 and figure 19 were used to indicate the state of the picogrid on each node. This alerts the user to manually connect or disconnect loads in order to avoid unnecessary trips due to over voltage or under voltage states. As shown in figure 23, these five state LEDs are supplied by the 24V power supply on the load node whereas sources and storage nodes are supplied by the 24V-12V DC regulators. Each LED is connected to a PLC relay which controls the LED switching depending on the PBV. A voltage divider circuit is used at the 24 V source to limit the current through the LEDs.

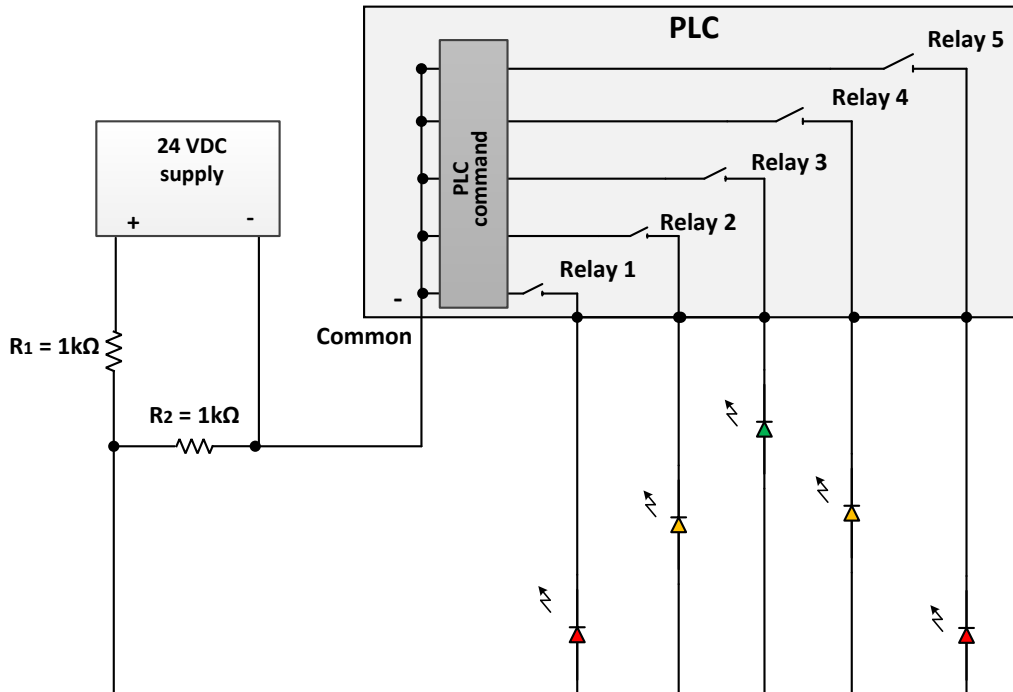


Figure 23: PBV LEDs connection to PLC relays

5.3.6. Solar/ Wind Regulator Knobs

These knobs shown by the photograph in figure 15 were used on both solar and wind nodes to regulate the dimmable light and the motor's power respectively. This in turn allows the dimmable light and the motor to replicate a PV panel and a wind turbine respectively. As shown in figure 24, the knobs are basically potentiometers connected to the grid and PLC. The PLC provides a reference voltage to the flyback converters which control the motor and dimmable light.

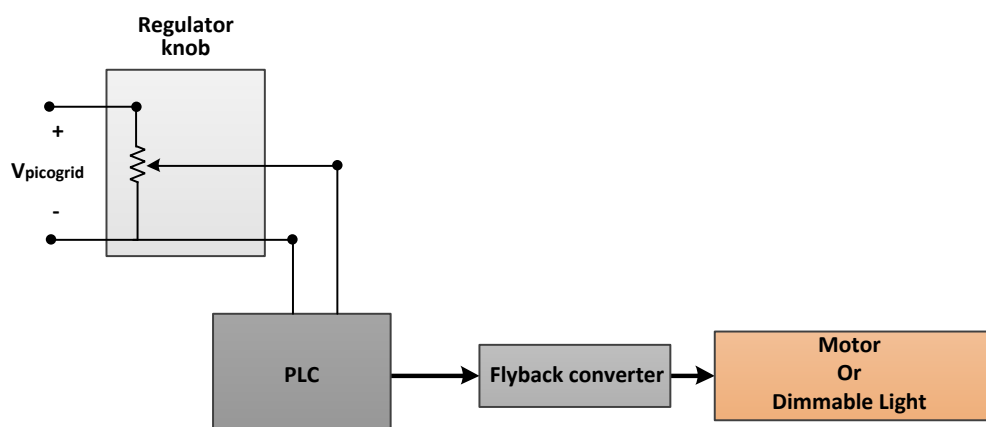


Figure 24: Solar/Wind regulator Knob

5.4. Other Required Components

5.4.1. HMI Display Panel

This display panel communicates directly with the PLC via Ethernet port as detailed in Appendix F. This panel is dedicated to the storage node as shown by the storage node photograph in figure 18. Its function is to act as a virtual battery by displaying battery properties such as state of charge, charging and discharging current. This is explained in detail in section 6.6 dealing with the storage node control. It can thus be said that the HMI replicates a real battery as it can display the battery percentage as well as the charging and discharging properties of a storage node.

5.4.2. Network Switch

As shown in figure 25 and the overall photograph in figure 26, two network switches were used to allow each of the four PLCs and the HMI to communicate with the host computer only when programming needs to be done. Each switch is unmanaged and has five RJ45 network ports [49]. Two switches were thus required in order to network all six devices together. Each PLC was assigned its own static IP address to communicate with the host computer. Details on setting up each PLC's communication for programming can be found in the node user manual in Appendix F.

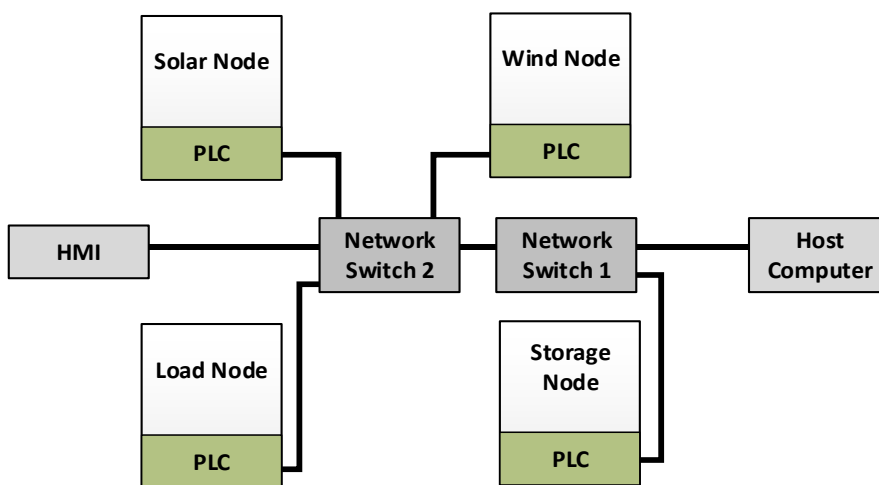


Figure 25: Star topology network connection between PLCs, HMI and host computer

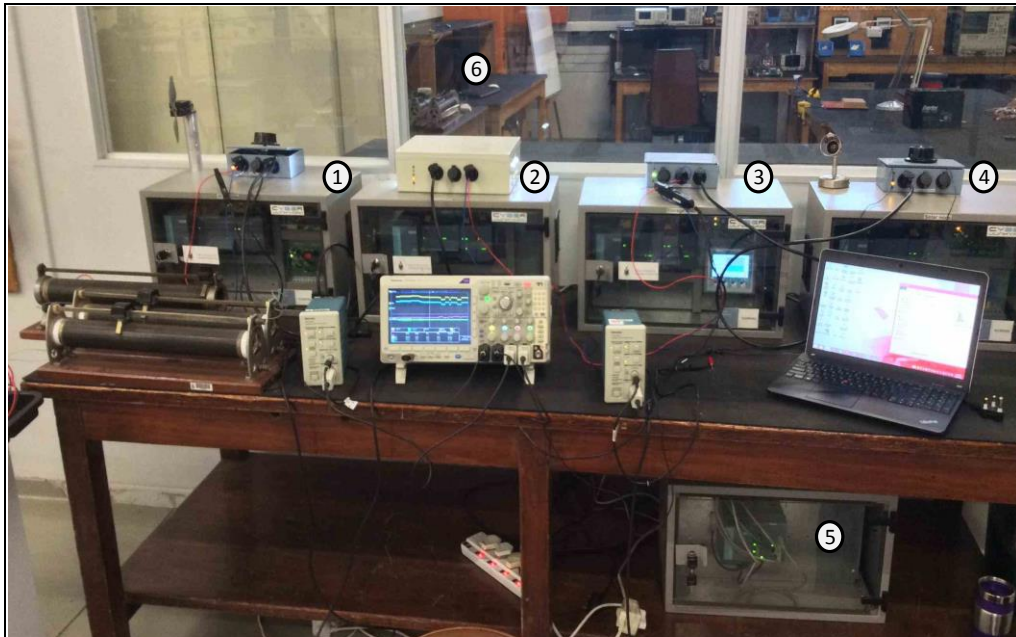


Figure 26: Picogrid Star topology network picture

Where: 1 - Wind node; 2 - Load node; 3 - Storage node; 4 - Solar node; 5 - Network switch;
6 - Host computer

5.5. Summary

This chapter has looked at the hardware composition of each of the demonstration nodes of the picogrid. Details on how power and information flows between a node's components have been discussed. For demonstration purposes, solar and storage node nodes are equipped with dimmable light and motor respectively which are controlled by regulator knobs. By regulating these knobs, the bus voltage can be set to any grid state. A storage node is also equipped with a touch display panel that replicates a real battery for the node by displaying different battery properties. The next chapter looks at the software implementation of the control algorithm on each node's controller.

6. Control System and Protection

6.1. Introduction

Each of the demonstration nodes discussed in chapter 5 has a unique control algorithm that complies with the grid code. This chapter provides detailed software implementation of each of the four demonstration nodes by looking at the control algorithms as well as the different protection schemes applied to the system.

6.2. Control Structure Overview

A Picogrid utilizes a decentralised control scheme with each node having its own controller. This makes it more suitable compared to a centralized control system which would malfunction if the main controller malfunctions. A picogrid's control system resembles the droop control algorithm for microgrid systems by using the bus voltage as the reference point for control [34], [36], [50-52] and current limiting for controlling the load current. The control system of a picogrid is structured in three different ways: primary, secondary and tertiary controls. Primary analog control limits the load current by maintaining the flyback converter in its continuous mode of operation. This in turn protects the system from short circuits which may lead to malfunctioning of internal components. Secondary analog control is responsible for controlling the output voltage of the flyback converter by providing a reference voltage value to the PWM controller. This is done via an opto-isolation amplifier so as to maintain the voltage isolation between the primary and secondary side of the flyback converter.

As shown in figure 27, primary and secondary controls form analog control scheme as they have a fixed control algorithm and occur within the flyback converter circuit. Tertiary control brings in the flexibility of digital control by utilizing PLCs which can take different commands. The control platform structure and description can be found in Appendix P, figure P1.

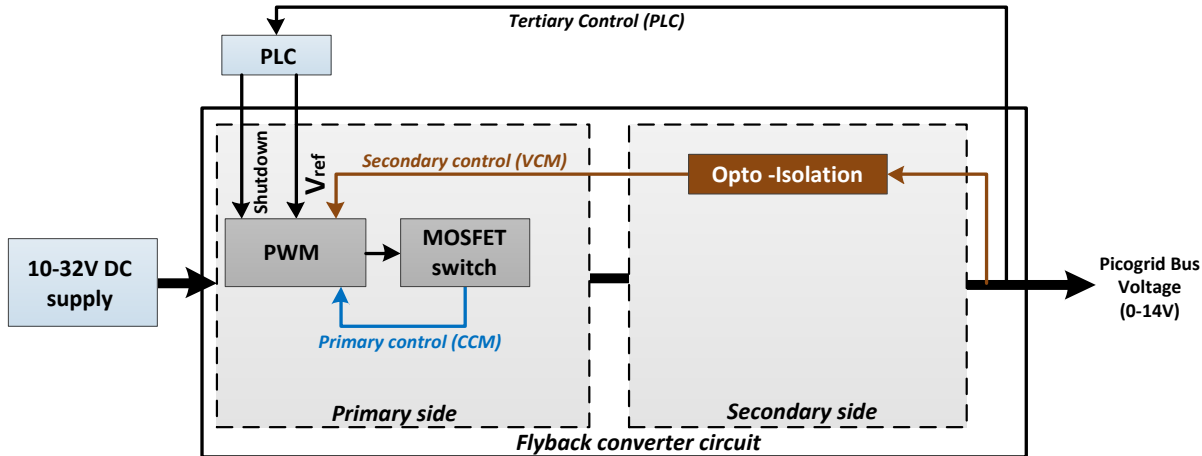


Figure 27: Control system structure of a source and storage node

As seen in figure 27, analog control occurs within the flyback converter circuit with its processing time limited by the PWM controller processing speed. This is around 20 microseconds as the switching process occurs at a frequency of 42.7 kHz. The amount of time that each digital controller takes to make a decision is always greater than the analog control processing time. This ensures that primary, secondary and tertiary control schemes are always executed in that order for better protection and maintaining stability. One of the benefits of using digital control is the flexibility and ease of modifying the control algorithm used, something which is complex with analog control as electrical components would need to be changed.

6.3. Common Control Algorithm

A Picogrid Bus Voltage (PBV) LED indicator algorithm shown in figure 28 was duplicated for each node. The algorithm deals with only switching LEDs ON/OFF depending on the state of PBV. The PLC code can be viewed in Appendix N.

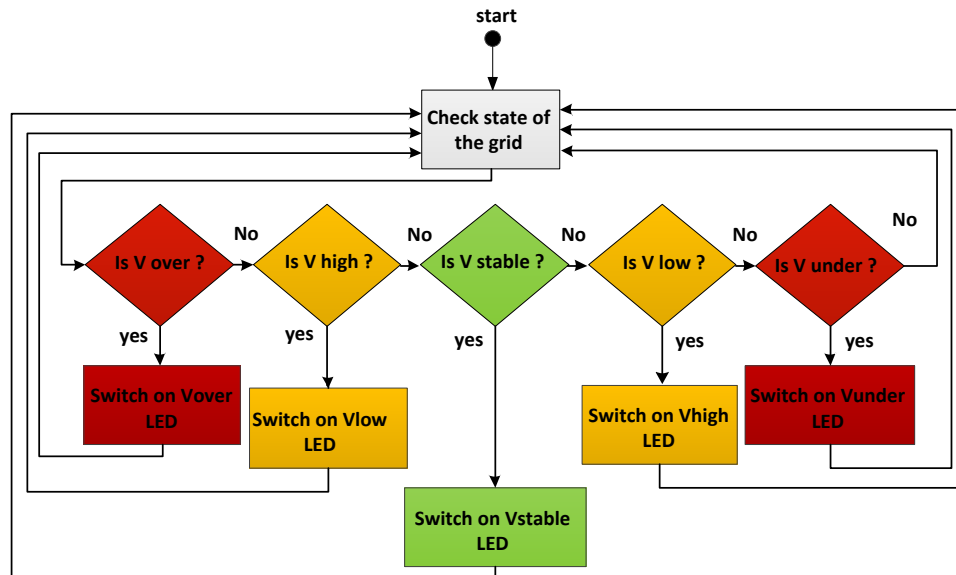


Figure 28: PBV LED indicator Algorithm

6.4. Solar and Wind Node Control

Solar and Wind nodes have the same control scheme utilizing the three control modes; primary, secondary and tertiary controls.

6.4.1. Primary and Secondary Control Algorithms

As shown in figure 29, the switching circuit of the flyback converter (being a MOSFET) performs the primary control of limiting the load current. K_{I_MOSFET} represents a constant proportional value of the varying MOSFET current, which is the current limiting resistor.

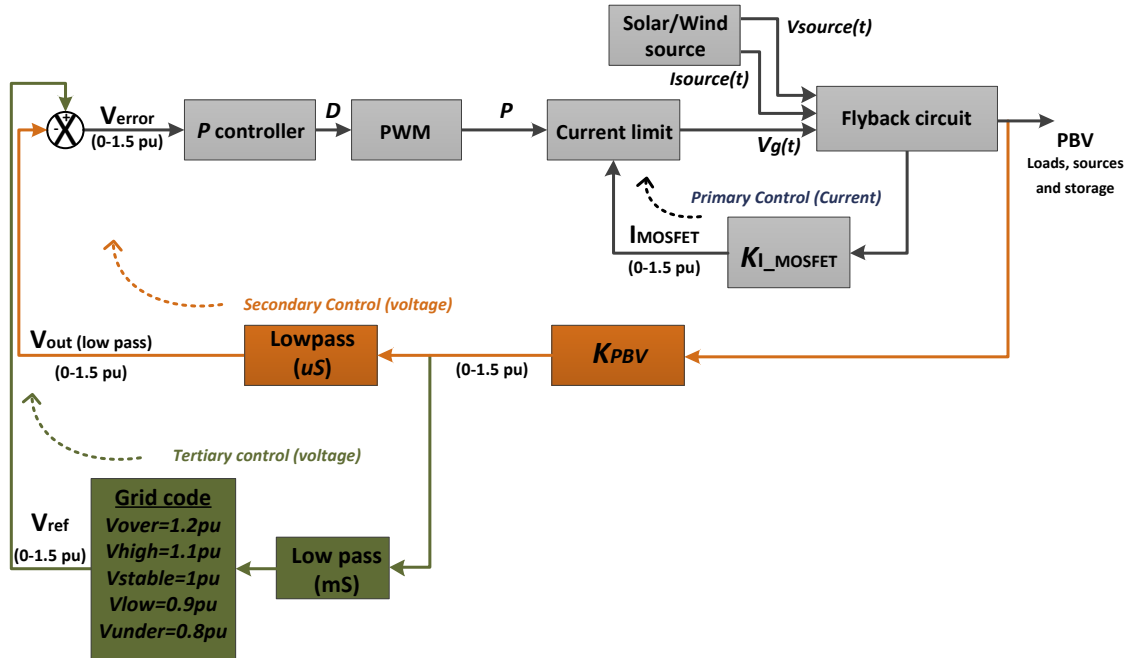


Figure 29: Source node control blocks

In figure 29, secondary control loop obtains a scaled proportion of the PBV (K_{PBV_t}). The constant K is set by having a voltage divider from the output of the flyback converter circuit. The procedure used to determine the constant K for the current limit is detailed in Appendix C page 5 to page 7. The error signal goes through a low pass filter before being sent to a PWM error amplifier which performs proportional control by amplifying the error signal. PBV is represented as a per unit value with 1 per unit value being the stable operation of 12V. The error amplifier then produces an output voltage for compensation from the resulting error voltages obtained by both secondary and tertiary control loops. This signal is then modulated by the PWM comparator before being sent to the power stage of the flyback circuit. Ideally MPPT controllers are encouraged over any other solar PV controllers [50-52] such as the PWM controller used, but this was chosen due to its lower costs and easier implementation compared to MPPT controllers. The error amplifier circuit is discussed in Appendix C page 4.

6.4.2. Tertiary Control Algorithm

From figure 29, a PLC performs tertiary control by providing a reference voltage to the PWM's error amplifier depending on the state of the bus voltage (PBV). As shown in figure 20, the measured voltage gets converted from the PLC's word to real value before going through the “gridcontrol” function. Each state of the grid is recorded in the solar or wind

control functions which are responsible for changing the PBV through the regulator knobs. These functions together with all other PLC source codes for solar and wind node algorithms are provided in Appendix J and Appendix K respectively.

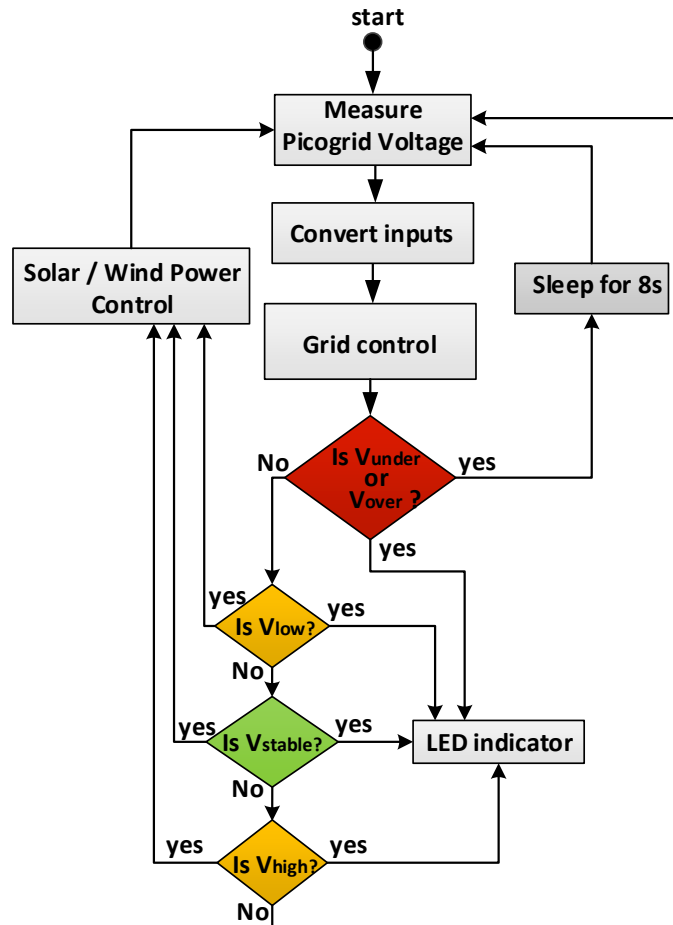


Figure 30: Tertiary control flow chart algorithm

6.5. Load Node Control

The control system for conditional loads operates in a similar manner as the utility's load shedding routine which occurs when there is stress on the grid caused by an overload. As shown in figure 31, the concept of load shedding is realized by having four loads connected or disconnected from the grid depending on the state of the PBV. It is shown in chapter 7 how the load shedding reduces the load current and hence providing more stability as the voltage. This offers more stability to the grid by reducing the number of node resets as the number of times the system goes into under voltage is decreased.

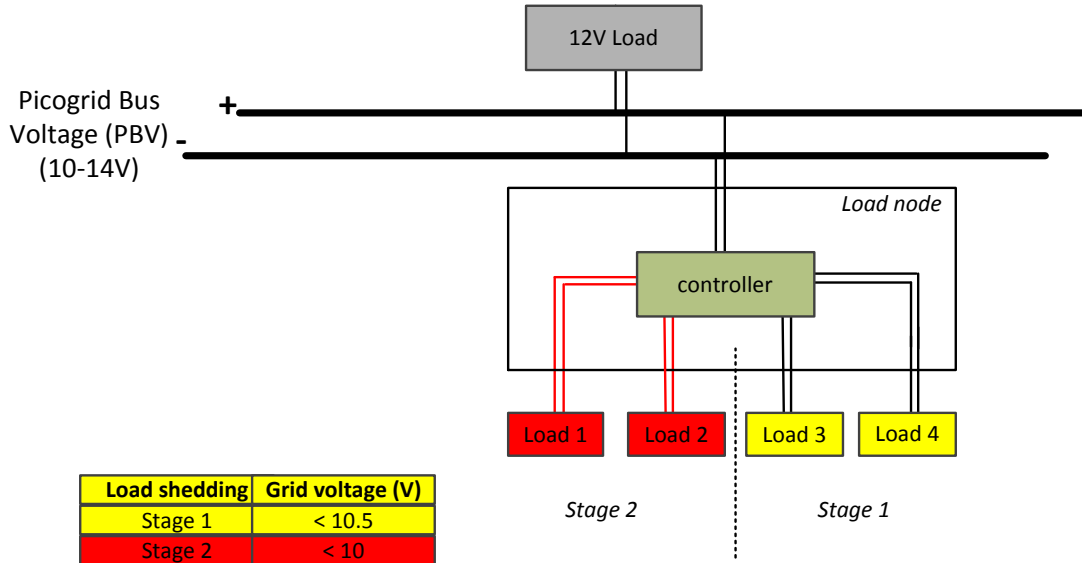


Figure 31: Load shedding concept

As shown in figure 31, the first stage of load shedding is activated by switching off load 3 and load 4 when the picogrid voltage goes below 10.5V in the low voltage mode. When the voltage continues to decrease such that PBV is below 10V, the system activates stage 2 load shedding which switches off all conditional loads.

6.5.1. Tertiary Control Algorithm

A load node only performs load shedding depending on the PBV state. The node does not have a flyback circuit and thus it only performs digital control based on the state of the picogrid. The algorithm of a control system for conditional loads is shown in figure 32 below. The first command performed by a load node is to check whether all conditional loads are off before measuring the grid voltage. This is because having all conditional loads off implies that the node is in sleep mode due to under voltage or over voltage state. This condition of checking whether conditional loads are switched off is processed faster by the controller than having to measure the grid voltage first in order to determine the node's state. The controller then connects all loads if they were initially off. If one or more of the conditional loads are on then it implies that the picogrid is active in any of the three states: low voltage, stable or high voltage state. The controller then proceeds to measure the grid voltage and then applies the necessary load shedding in low and under voltage states. When the grid is in stable or high voltage states, the controller connects all the conditional loads as there is enough power being generated. Details on the implementation of the control algorithm in the controller platform

can be viewed in Appendix P. This appendix provides all the function declarations and descriptions of key functions used to achieve the node's functionality. The source code with software implementation can be found in Appendix L.

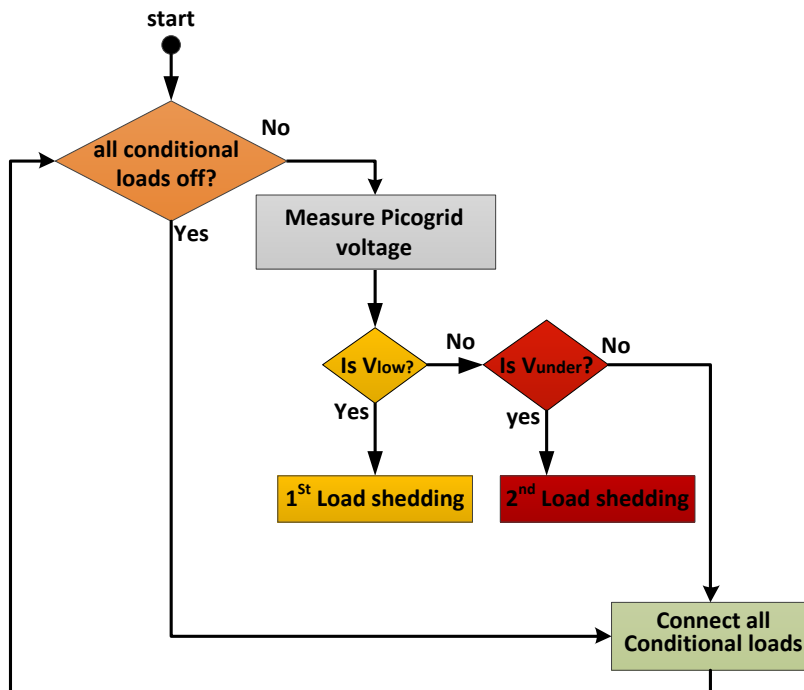


Figure 32: Load node control Algorithm

6.6. Storage Node Control

6.6.1. Primary and Secondary Control Algorithm

Storage node control has all the three modes of control applied to it as shown in figure 33. The only additional functionality that the node applies is using the state of the picogrid voltage to switch between sourcing and sinking current so as to resemble a real battery's charging and discharging properties based on the battery's state of charge. From figure 33, five modes of control are achieved by the storage node; primary, secondary, tertiary 1, tertiary 2 and tertiary 3. Primary, secondary and tertiary 1 controls have the same logic as the source nodes. Tertiary 2 and tertiary 3 controls are used by the controller to switch between sinking and sourcing current in the picogrid respectively.

6.6.2. Tertiary Control Algorithms

Depending on the state of the bus voltage, a controller will either switch between tertiary 2 or tertiary 3. This occurs in a time less than other control switching times (in milliseconds). From figure 33, when the bus voltage is in high or over voltage states, the controller closes the relay switch so as to allow the excess current to charge the battery. However, since there is no battery present, the current gets sunk into constant resistor R_{sink} and the sinking current value gets displayed on the HMI screen. Trickle-charging versus rapid charging is defined in the controller depending on the state of charge. Details of the HMI display for sinking and sourcing currents are provided in the node user manual - Appendix F. When the voltage state is in low or under voltage, a sourcing relay is closed so as to allow the storage node to supply constant power to the picogrid so as to assist it to go back into a stable state.

Figure 34 shows the control algorithm flowchart implementation of the tertiary controls using the provided controller. From this figure, there are two types of controls: storage grid control and grid control as detailed in Appendix P, section 3 and figure p6. The storage grid control performs the same function as the source nodes grid control of checking what state the picogrid is in and responding by switching on the corresponding PBV LED. The grid control on the other hand is responsible for connecting the node to the grid when the bus voltage drops below stable region or the battery's State Of Charge (SOC) is above 30%. This allows the node to act like a backup system that supports the grid when in critical state. This control thus enables the node to source current to the grid as per tertiary 3 control.

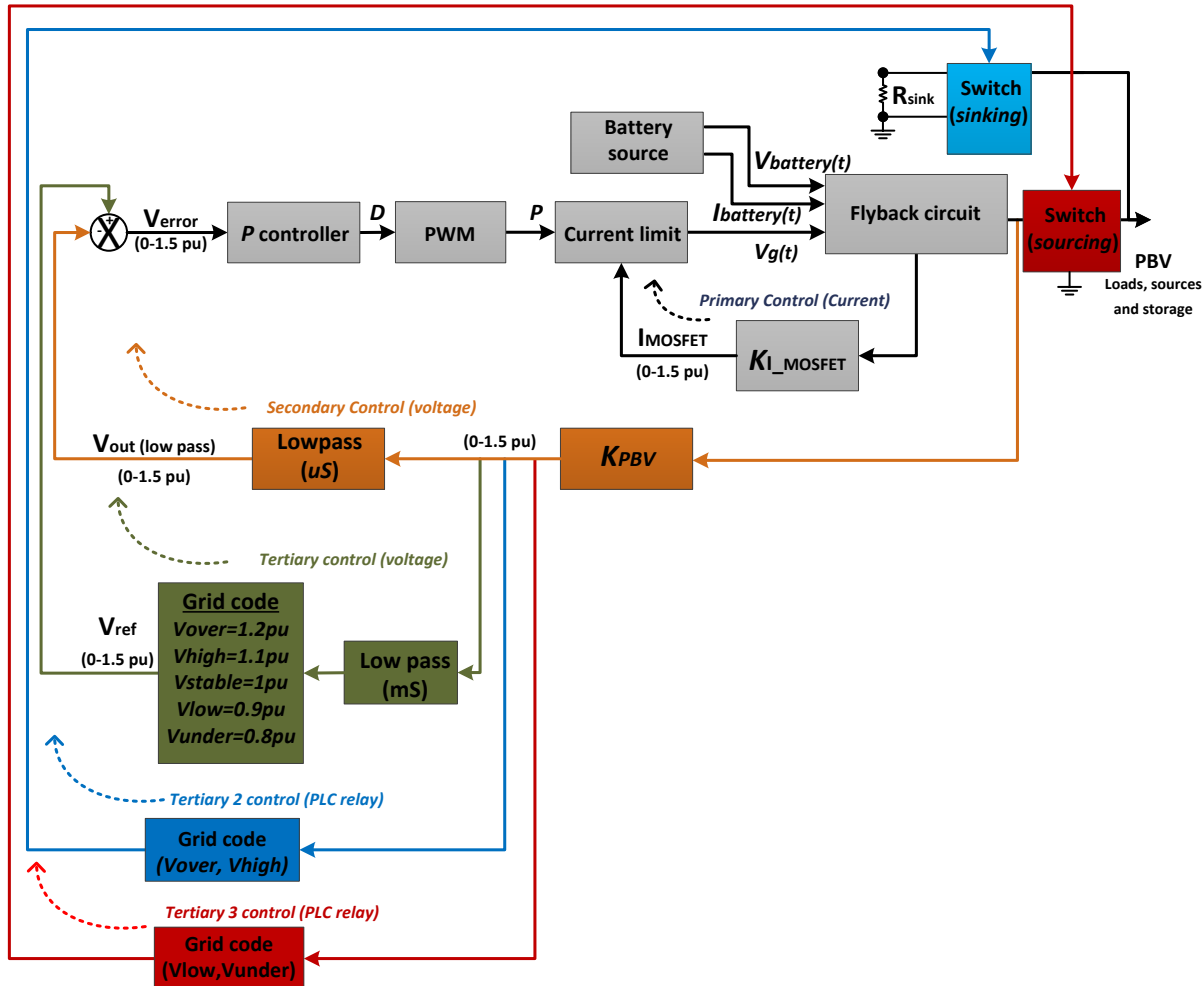


Figure 33: Storage node control blocks

From figure 33, the grid control function also disconnects the node from the grid in the event of a short circuit or when the grid state is in under or over voltage. The node then goes into sleep mode for 8s before checking the bus voltage state again. This 8s were set randomly in order to make testing easier.

When the picogrid bus voltage is in high voltage state, the sinking resistor connects to the grid in order to absorb the excess power with the aim of bringing back the picogrid to a stable state. If the resistor does not draw enough current the system goes into over voltage which results to shut down. The minimum value required for the sinking resistor is provided in Appendix B.

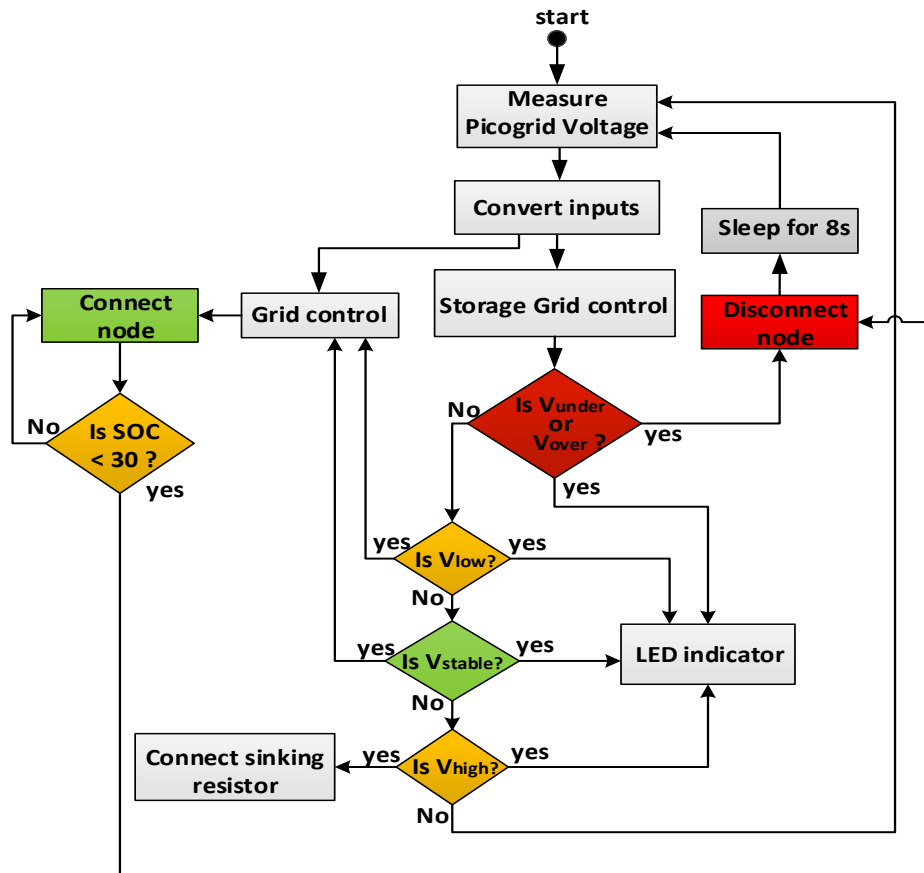


Figure 34: Storage node control algorithm process flowchart

6.7. Summary

A form of droop control similar to that used in AC systems droop control of voltage and frequency has been implemented on sources and storage nodes with each node having a decentralized control scheme for controlling both voltage and current. The control scheme is divided into three control algorithms; primary, secondary and tertiary controls. These control algorithms were defined based on how fast each algorithm gets executed with analog control occurring faster than digital control. The next chapter tests the control algorithms by looking at the tests performed on each node and the overall system combined.

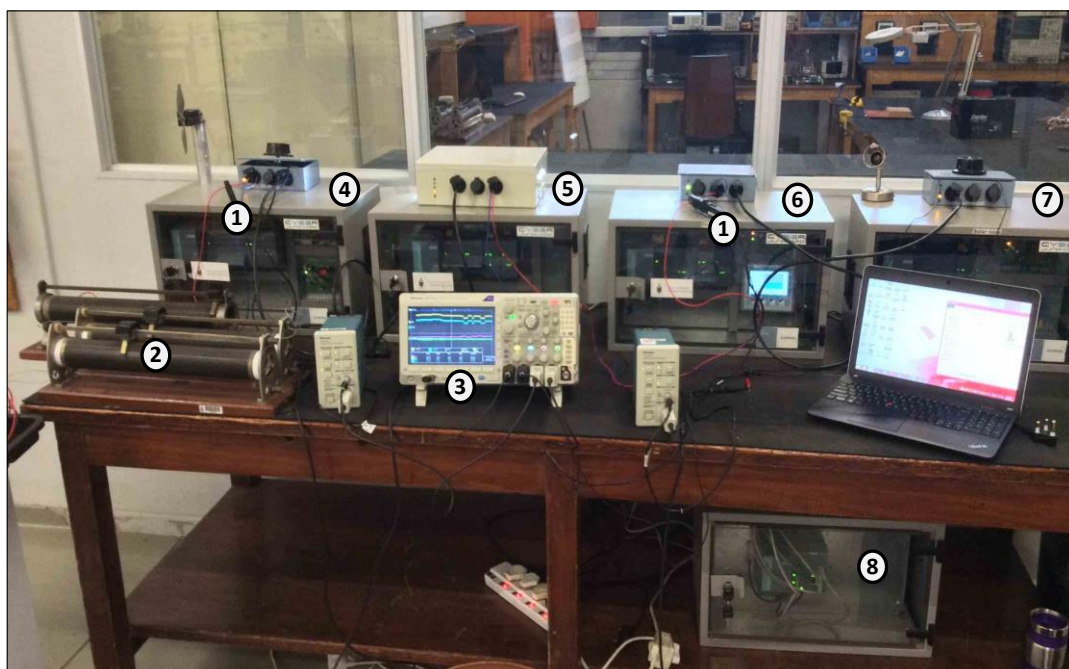
7. Picogrid Tests and Results

7.1. Introduction

The success of this research lies in the outcomes obtained from laboratory testing of the Picogrid concept. These tests will be the key elements used to answer the research question on whether improving the control and protection of the picogrid enhances scalability. This chapter thus looks at testing the application of the control algorithm discussed in the previous chapter. The protection scheme of the system will also be tested. The outcome will therefore involve proving that a picogrid is scalable and can recover automatically from faults through detailed tests and analysis of the results obtained.

7.2. Test Setup

Individual node tests were firstly performed before testing the system as a whole. The laboratory test circuit picture is shown in figure 35. The corresponding test circuit diagram is shown with each test conducted.



Where:

① Oscilloscope Current probes

③ Mixed domain Oscilloscope

⑤ Load node

⑦ Solar node

② Variable loads

④ Wind node

⑥ Storage node

⑧ Network Switch

Figure 35: Picogrid laboratory test setup

7.3. Node Tests

Each node's start-up characteristics together with its response to different bus voltage levels and faults on the grid were tested. The following tests were performed on the nodes in the research laboratory.

- Open Circuit (OC) and Short Circuit (SC) tests with no load
- Over voltage and Under voltage tests
- Load tests on individual nodes(current limiting tests)
- Load shedding tests
- Sudden removal or connection of a heavy load

All the above tests were conducted in order to determine the level of protection designed in the picogrid. Only the load shedding test will be verifying load automation by automatically shedding conditional loads when the bus voltage goes below critical levels in the low voltage state.

7.3.1. Open Circuit Voltage and Short Circuit Current tests with no load

Open Circuit (OC) and Short Circuit (SC) tests were performed individually on each node without any load connected in order to observe the magnitudes of the sudden voltage and current rise when an open circuit or short circuit faults occurs respectively. The aim of these tests was to verify the safety features of the picogrid when sudden electrical faults arise and how the system automatically self-recovers when faults occur. The test setup diagram for solar, wind and storage nodes is shown in figure 36.

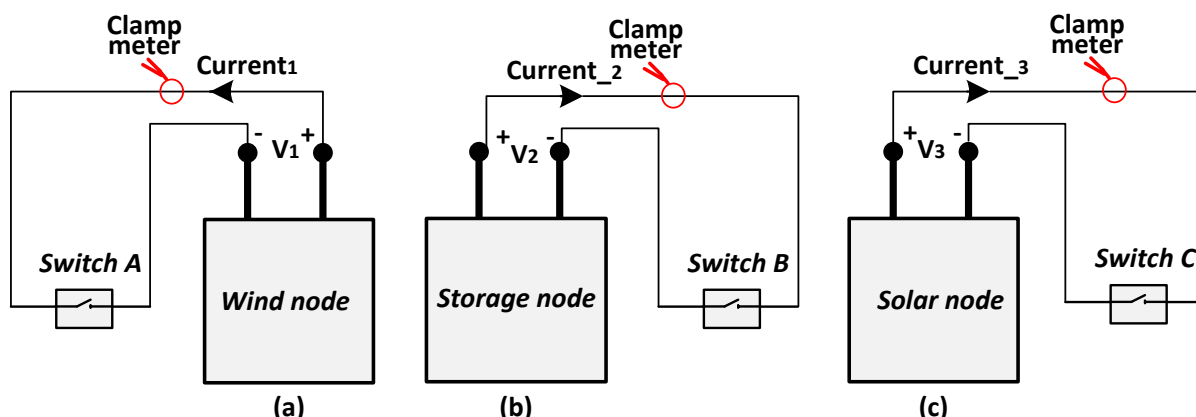


Figure 36: OC and SC test setup diagram for; (a) wind, (b) storage and (c) solar node

From the figure, each switch was operated manually at a slow time (in seconds) the fastest possible time an end user would operate the picogrid cannot be any lower than seconds.

As shown in figure 37 below, Switch A of a wind node was closed after 27s for 4s. A short circuit was immediately observed with the voltage (V_1) dropping down to zero. The SC current however develops a sharp spike at exactly the same time the SC is introduced. This sharp spike of about 4.8A drops down to zero in less than a second before the node goes into sleep mode and attempts to restart after 8s. This spike is caused by the slower response time (discussed in section 6.4) that it takes the digital control to limit the sudden rise in current resulting from the DC to DC converter's faster analog control.

As shown in figure 38 and figure 39, switch C and switch B were closed at 32 and at 47 seconds for the solar and storage nodes respectively. The same duration time of roughly 4s was applied to these switches. For a solar node, figure 38 shows the similarities between the voltage (V_2) and current (Current_2) graph to that of a wind node graph. The current spike is also at 4.8A and it takes the node 8s in sleep and restart mode. A storage node however presents different results as depicted from figure 39.

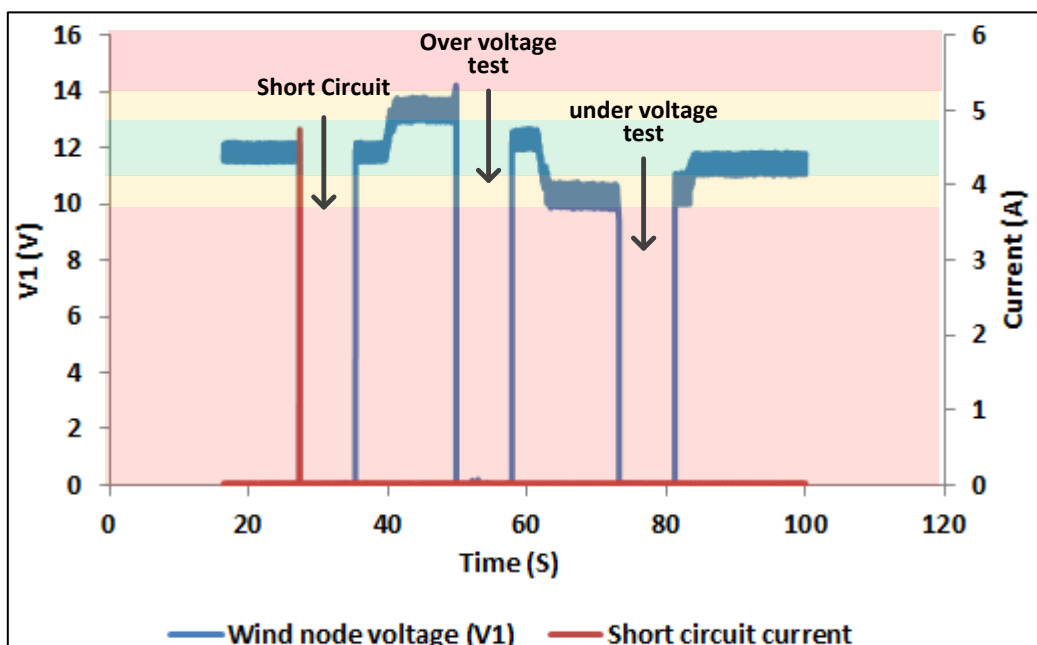


Figure 37: Wind node OC voltage versus SC current, OV and UV tests

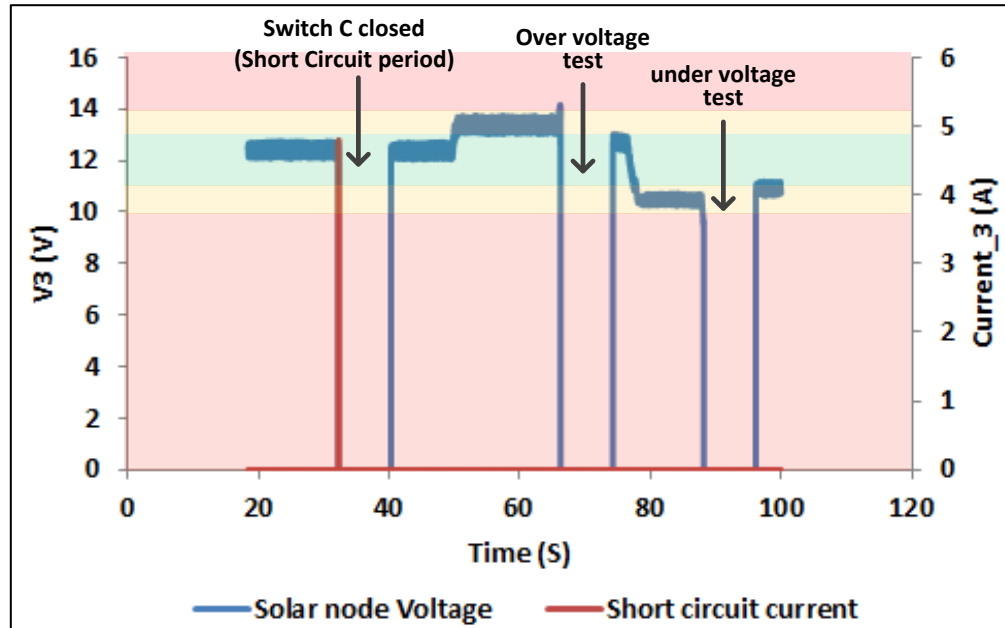


Figure 38: Solar node OC voltage versus SC current

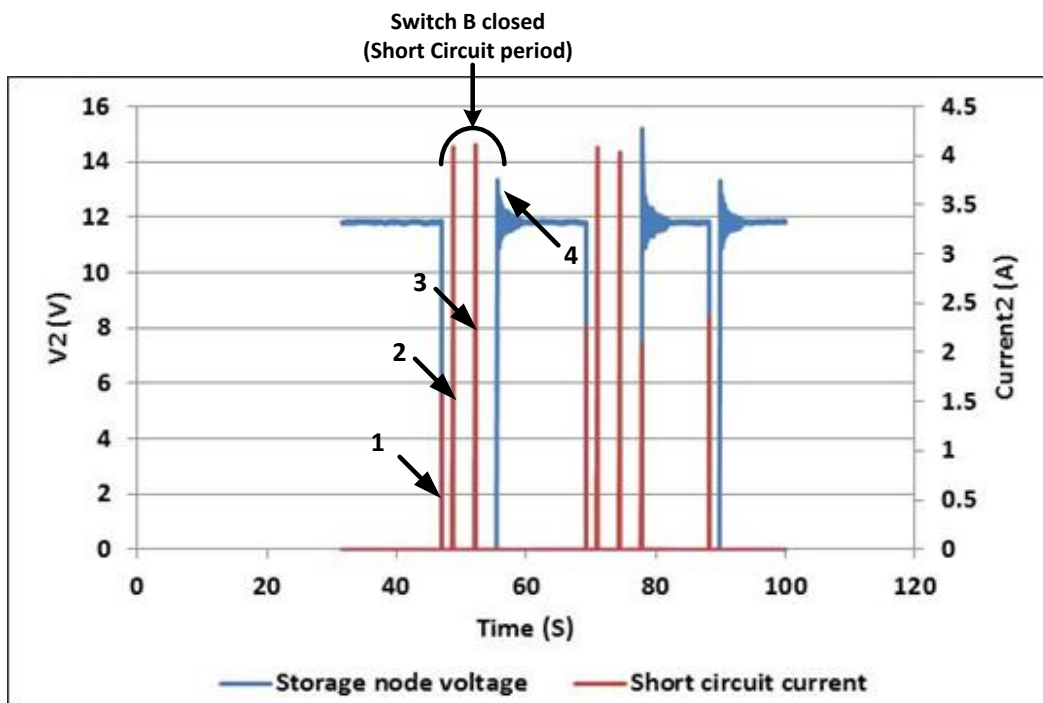


Figure 39: Storage node OC voltage versus SC current

From figure 39, four transient spikes (indicated by numbers) can be observed;

1. Short circuit current: This is due to the slower processing speed of the digital control which raises the current due to the zero voltage than the DC-DC converter's faster speed of increasing the current when a short circuit occurs as discussed above.
2. And 3. Both spikes result from the attempted restart of the node whilst there is still a short circuit present. This is because unlike a solar and a wind node, a storage node's sleep mode resulting from short circuits is activated by the DC-DC converter (analog control) of the node and not the PLC (digital control). The DC-DC converter used for the storage node had an improved current limit (Current Control Mode) than the source nodes as discussed in chapter 5 section 5.3..
4. Voltage spike caused by the sudden removal of a short circuit: This is resulting from the slower PLC's digital control time that it takes to stabilise the voltage than the time it takes for the analog control of the DC-DC converter to raise the voltage immediately when the short circuit is cleared. This can be reduced by additional damping resistors to the converter circuit.

7.3.2. Under Voltage and Over Voltage tests

These tests were performed on source nodes together with OC and SC tests discussed above in figure 37 and figure 38. The aim of these tests was to prove that sources and storage nodes go into sleep mode whenever the bus voltage is in over voltage or under voltage mode shown in both figures. This not only provides safety voltage limits but also makes sure that there is always sufficient power available on the picogrid when faults are not present.

7.3.3. Load tests on Individual Nodes

The aim of the load test was to determine the maximum load that each node can withstand in the stable operating region (11V-13V) before dropping to other PBV states. These tests also provide the electrical characteristics (voltage, current and power rating) of each source and storage node. As shown in figure 40, a varying load of ($0-25\Omega$) was connected to each source and storage node and the resistance was decreased until the node trips and goes into sleep mode as a result of attaining its maximum output current. The time taken for the node to restart was then recorded.

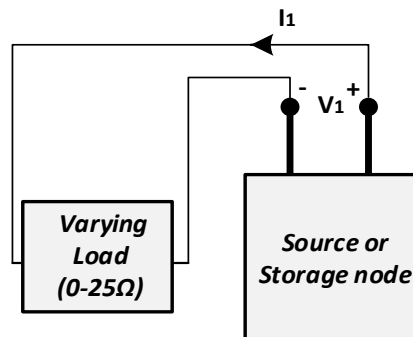


Figure 40: Load tests setup for each node

Wind Node: The load was first connected to a wind node then voltage and current measurements were recorded. Figure 41, shows the resulting graphical presentation of the voltage and current waveforms versus time.

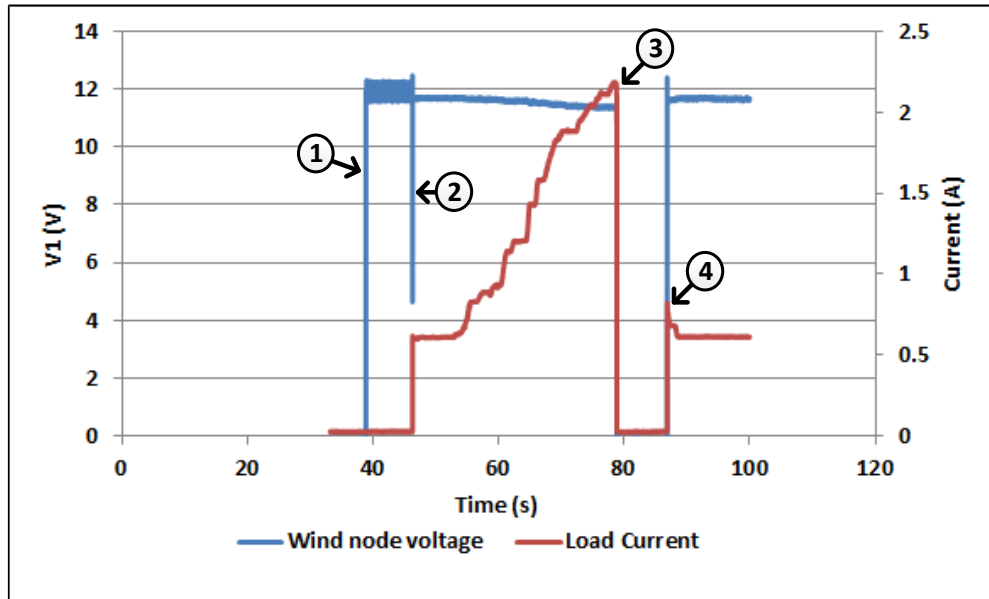


Figure 41: Wind node voltage and current waveforms against time, with a varying load

Both voltage and current measurements were recorded against time. A more clear graphical analysis of the voltage versus current representation was extrapolated from the waveform in figure 41 to form the current versus voltage waveform shown in figure 42. Both graphs (figure 41 and figure 42) have the exact labelling from 1 – 4 in order to ease comparison.

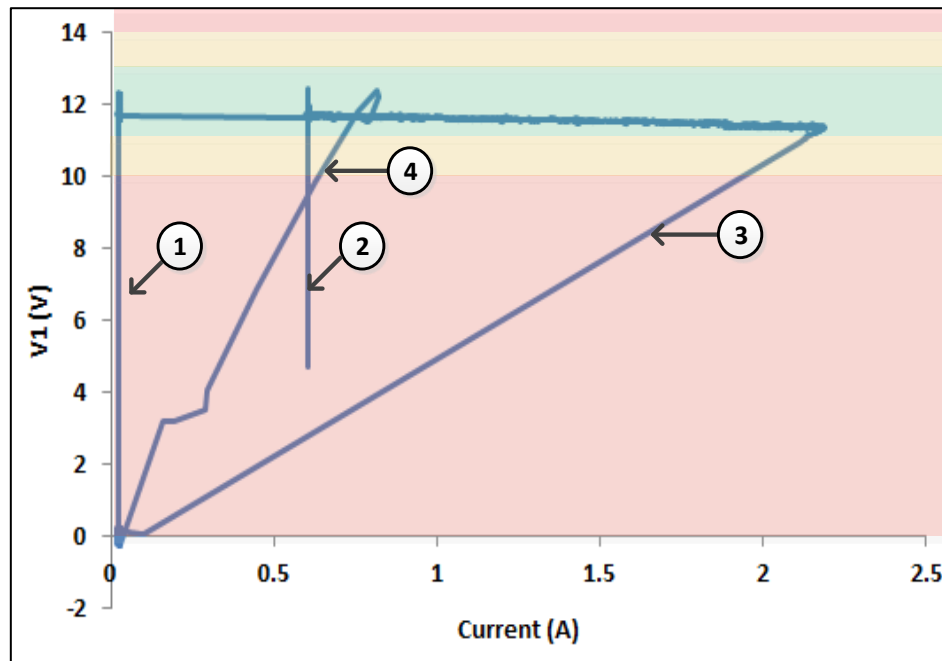


Figure 42: Wind node voltage versus current graph of the varying load

From the figure, the shaded regions show the state of the PBV. The following four indicated conditions occur in order;

1. At 38s in figure 41, the wind node energises the picogrid and produces the bus voltage (PBV) which shoots immediately to the stable region as V_1 .
2. At 46s, the variable 25Ω load is connected to the node and the high rush in current causes the voltage to drop drastically to 4.68V. This is immediately corrected by the analog control of the node's DC-DC converter (within a second) before the digital control responds to tripping the node due to the voltage drop; a process that occurs slower than the analog control as discussed earlier. The node therefore does not trip but continues into stable mode. From 50s, the load resistance is reduced further until a threshold current is reached.
3. At 78s, the threshold load current of 2.19A that the wind node can supply is reached and this causes the node to trip. Both voltage and current drop to zero as shown by the figure. This proves that the node's Current Control Mode (CCM) for controlling the current limit performs satisfactorily.
4. At 86s, that is after 8s into sleep mode, the node restarts and goes into stable mode as required. It is worth to note that when the node shuts down, the load resistance is

manually increased (during the sleep mode) in order to observe whether the node automatically restarts as required.

Solar Node: The load was then connected to a solar node and the same procedure as with the wind node was followed towards obtaining the voltage (V_2) and current (current_2) graph shown in figure 43.

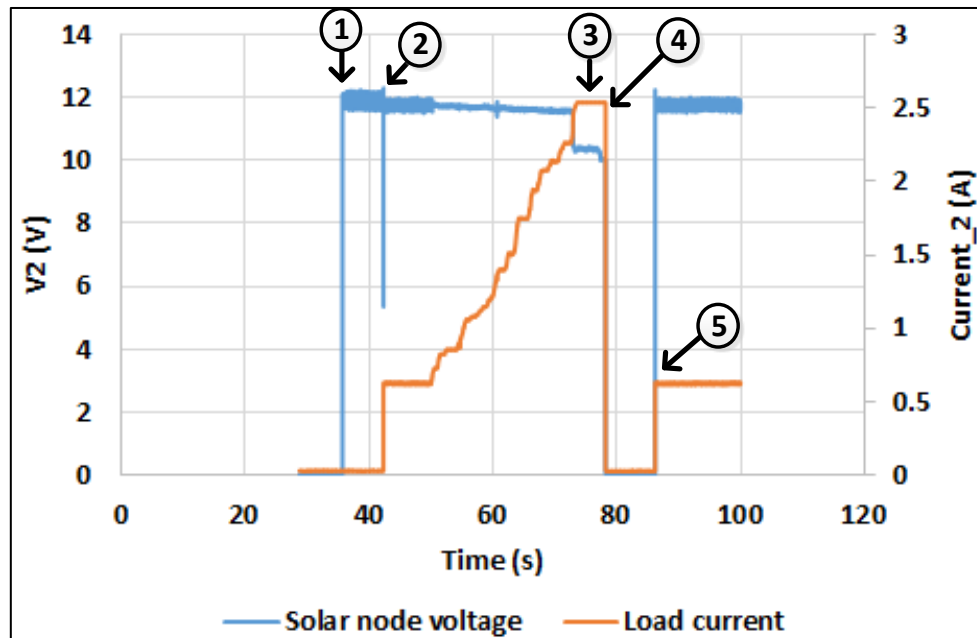


Figure 43: Solar node voltage and current graphs of a varying load

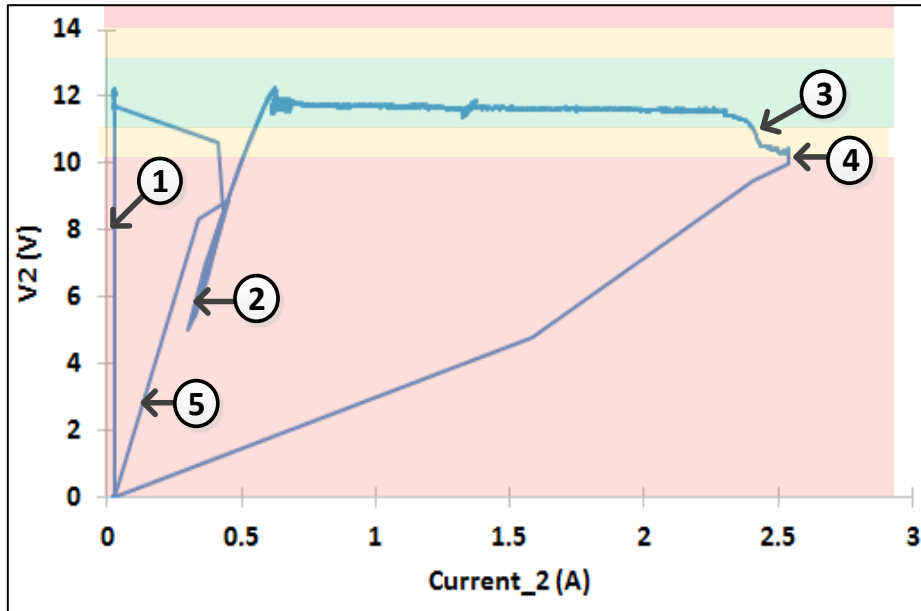


Figure 44: Solar node voltage versus current graph of the varying load

From both figure 43 and figure 44, the following conditions occur in order:

1. At 36s, the solar node starts and produces the bus voltage (PBV) which shoots immediately to the stable region as V2.
2. When the 25Ω load is connected at 42s, the node behaves just like a wind node by having its voltage (V2) drop sharply to around 5.35V. The node quickly recovers and attempts achieving a stable mode of operation. The varying load resistance was then gradually decreased until the voltage starts to drop at 72s.
3. From 72s to 78s, the bus voltage drops into low voltage mode as the load resistance is still manually reduced.
4. At 78s, the node's current limit is reached at 2.54A and hence both voltage and current drop to zero. The node goes into sleep mode for 8s as described previously before attempting to restart. It is worth to note that the maximum current supplied by this node before the voltage drops below stable region is 2.4A.
5. At 86s, after 8s of sleep mode, the node restarts and goes into stable mode.

Storage Node: Lastly, the load was then connected to a storage node which presented the graphs shown in figure 45 and figure 46. From the figures, a storage node can supply a maximum current of 1.72A, unlike the solar and wind nodes which can supply more than 2A. This is due to the different design versions of the DC-DC converter used for the nodes. As mention in chapter 4, although a storage node has the latest version (version 3), the inductor

used for its DC-DC converter goes into discontinuous mode earlier than the solar and wind node's inductors.

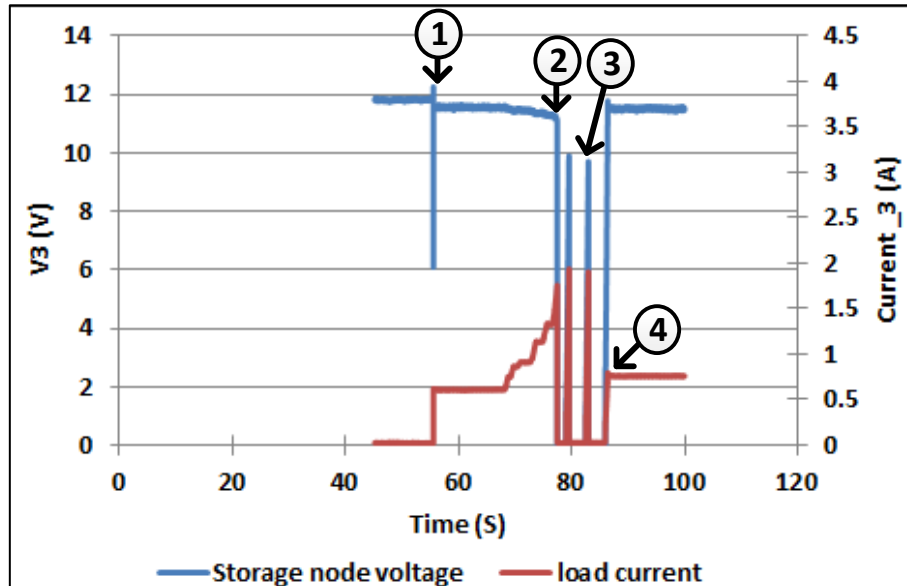


Figure 45: Storage node voltage and current graphs of a varying load

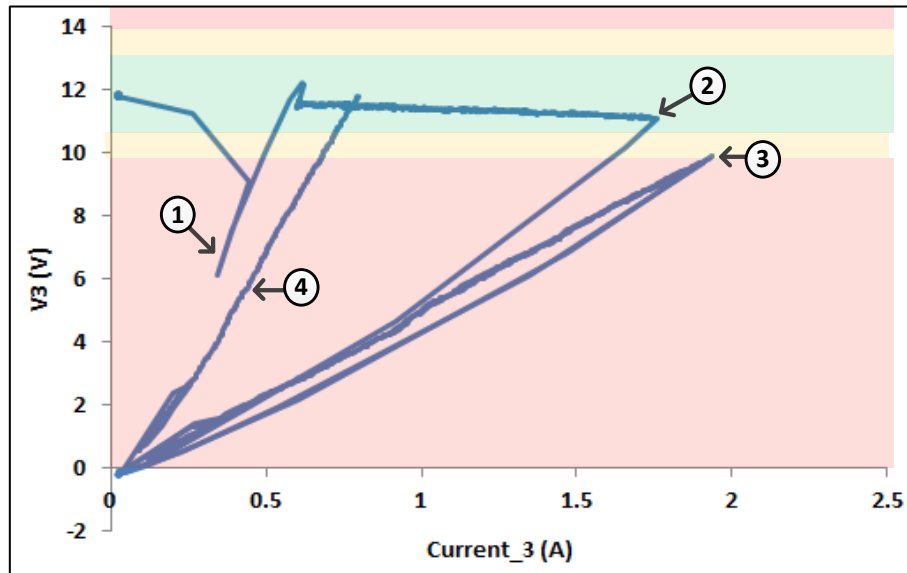


Figure 46: Storage node voltage versus current graph of the varying load

From both figures, the following conditions occur in order:

1. At 55s, the load is connected and this leads to the sharp voltage drop as observed previously on other nodes.

2. At 77s, a maximum threshold current of 1.76A is achieved in the stable region before dropping to zero and then into sleep mode.
3. During the sleep period, at 79s and 82s, the node attempts to restart by supplying a rush in current of 1.88A and 1.85A respectively. This shows that the node recovery from sleep is 3s as opposed to the solar and wind nodes 8s of sleep. The 3s as discussed earlier is because of an improved analog control of the storage node's DC-DC converter which controls the current as opposed to the utilised digital control. This further proves the improved DC-DC converter of the storage node which utilises a faster analog control using Current Control Mode (CCM) of the DC-DC converter.
4. At 88s, the node recovers from sleep after the load resistance has been increased and the node goes into stable mode as required.

From the above tests, a summary of each node's electrical characteristics can be tabulated in table 5.

Table 5: Node voltage, current and power ratings

Node	Voltage (V)	Current (A)	Power (W)
Solar	11.74	2.40	28.18
Wind	11.59	2.19	25.38
Storage	11.25	1.76	19.80
Total = 73.36			

From the table, a combined output power of 73.36W is generated by the sources and storage nodes of the picogrid. To prove that a picogrid's power can easily be scaled up, a system test involving all interconnected nodes was conducted later.

7.3.4. Load Shedding test

A Load shedding test was performed on the load node so as to observe whether conditional loads are switched off when the bus voltage goes below low voltage levels. A load node has both conditional and non-conditional loads as described in section 5.2.3. Figure 47 shows the test setup with a wind node used as the power source to the load node. Each of the eight resistive loads was then activated through its respective switch (switch 1-8) at different time intervals. The wind node's regulator knob was then varied so as to decrease the bus voltage to low voltage (<10V) whilst observing conditional loads. Figure 48 shows the graphical results obtained from the voltage (V_1) and current (I_1) measurements.

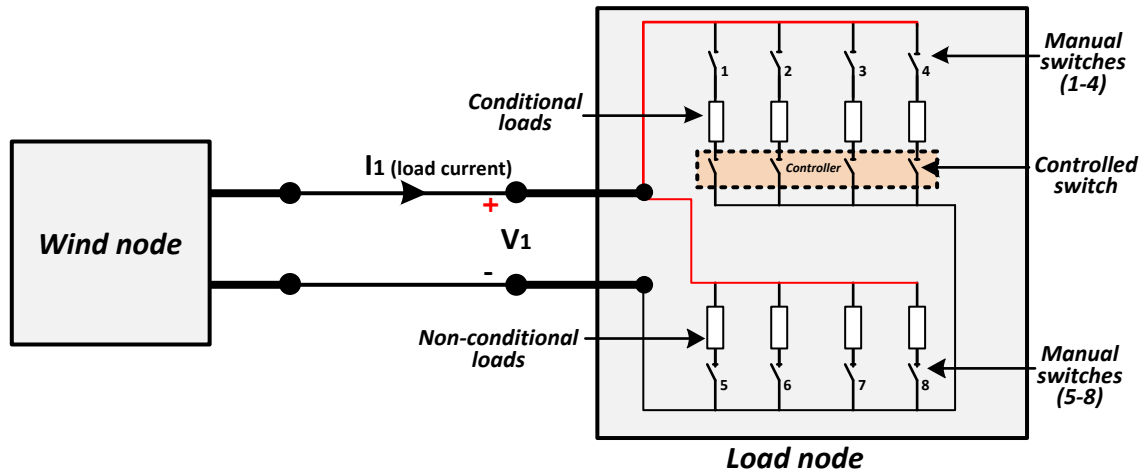


Figure 47: Load shedding test setup

Three tests were performed on the node;

1. Non-conditional load profile test – To verify the non-conditional load current.
2. Conditional load profile test – To verify conditional load current
3. Load shedding test – Where both conditional and non-conditional loads are manually switched on and the bus voltage reduced so as to trigger automatic load shedding.

Non-conditional load profile: After switching off all manual switches, the wind node was switched on and manual switches 5-8 were switched on in intervals of ten seconds as shown in figure 48. From the figure, voltage V_1 gets stabilised when each of the four loads connects to the grid as indicated by the thinning blue line. This is due to the wind node's open circuit voltage scenario explained earlier in the open circuit tests. All the loads together consume very little power as indicated by the total current recorded at point 8 (0.11A). These loads can easily be replaced with more power consuming loads ($>1A$) in the future for more load shedding tests. From the values obtained for V_1 and I_1 the load resistances were also verified as defined in the load node's schematic in Appendix G, figure G1.

The ringing presented by the voltage waveform is caused by noise from an almost open circuit source node. The voltage control mode during open circuit has noise as shown by the source node tests. The ringing reduces slowly with an increasing load as it becomes the damping resistor.

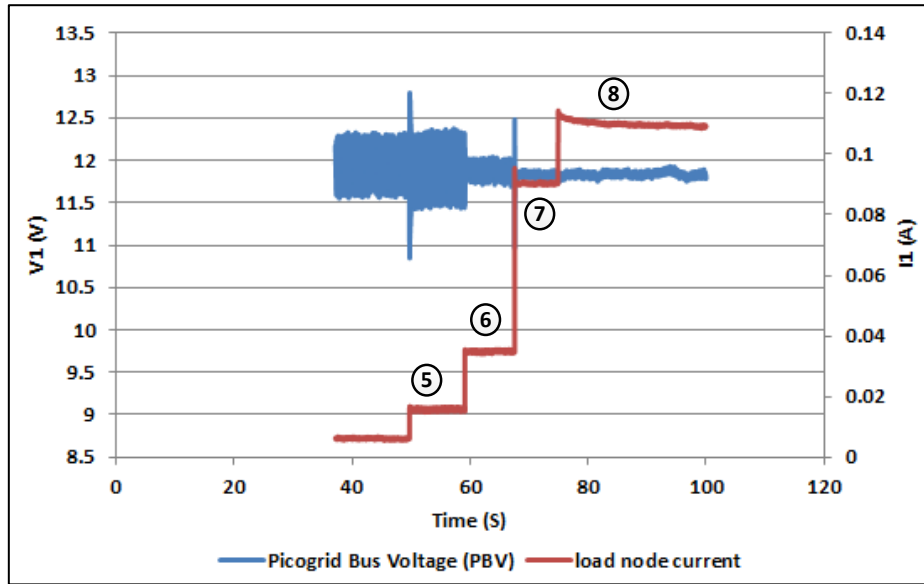


Figure 48: Non-conditional load profile

Conditional load profile: All switches were opened and then conditional loads (switch 1-4 shown in figure 47 above) switched on in 10s intervals. Figure 49 shows the resulting voltage and current graphs. Further tests which involved all conditional and non-conditional loads switched on so as to observe the maximum current drawn by the node were conducted and presented in Appendix O, figure O1.

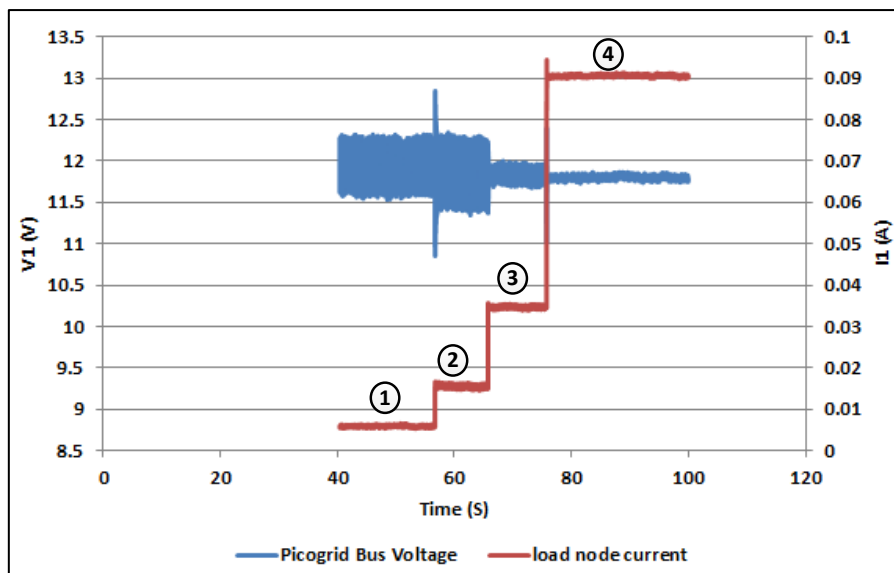


Figure 49: Conditional load profile

Load shedding test: From figure 47, load shedding is managed by the load node's controller by switching off conditional loads in two stages as described in the previous chapter. This test will thus prove that load shedding occurs automatically when the bus voltage drops to critical levels. All the switches shown in figure 47 were switched on so as to allow the load node to draw its maximum current. The wind node's voltage was then manually decreased using the regulator knobs whilst observing the LEDs for each switch. Voltage (V_1) and current (I_1) measurements were then recorded as shown in figure 50.

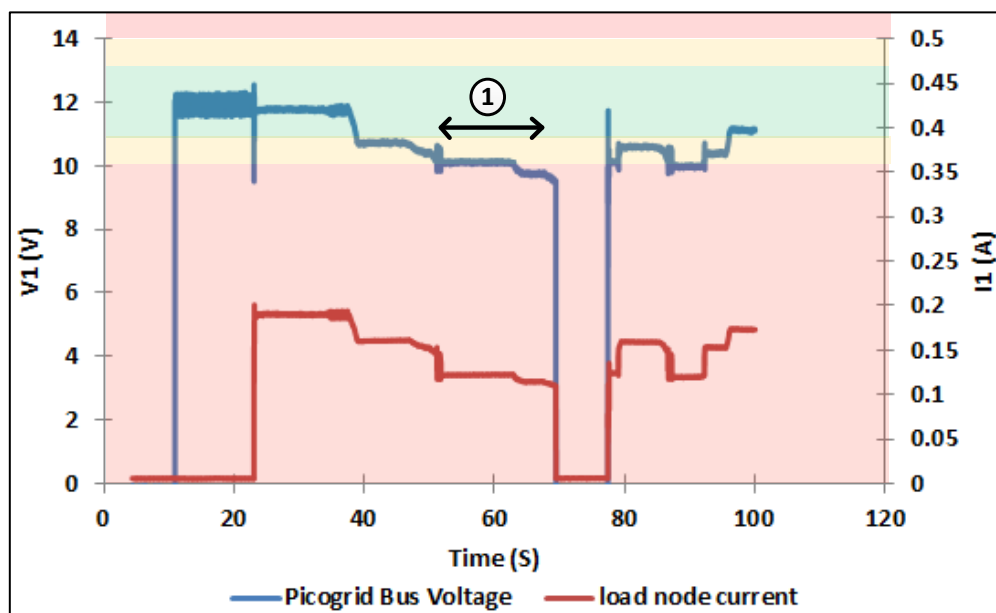


Figure 50: Load shedding test results

From figure 50, at 23s, the load node switches on and all the loads are connected. The wind node regulator knob is then slowly reduced in intervals of 10s until the first load shedding is observed at 51.15s. This is the region shown as 1. Figure 51 shows the zoomed portion of region 1 with the load current fluctuating before dropping by 75% whilst the voltage fluctuates between 9.8V – 10.6V. This happens because of the sudden 1st load shedding that suddenly reduces the load current causing the bus voltage to rise before being stabilised. This is discussed further in section 7.3.5.

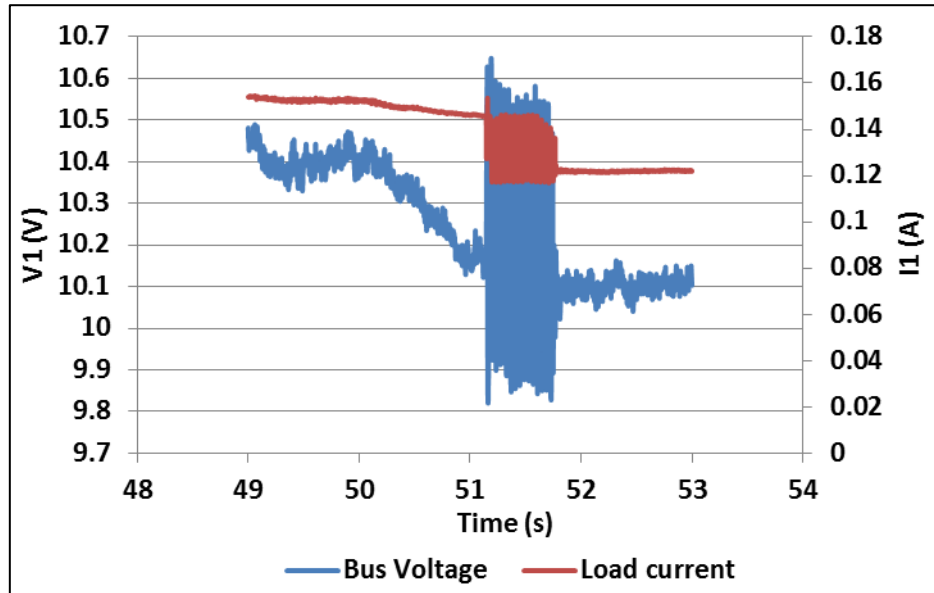


Figure 51: Zoom in at the 1st load shedding of figure 50

7.3.5. Sudden Removal or Connection of Load

A sudden OC resulting from removal or connection of a heavy load on a source or storage node would result in transient voltage spikes due to the slower time it takes the digital control to stabilise the voltage. This test was necessary for not only determining the magnitude of the transient spikes presented by sources and storage nodes but also for verifying that the nodes trip and reset when the voltage levels shoot above over voltage mode thereby proving that the protection scheme works.

The same test setup used in the load tests discussed earlier was used with the load however fixed to 15Ω . Figure 52 shows the voltage and current graphs of a storage node under the heavy load.

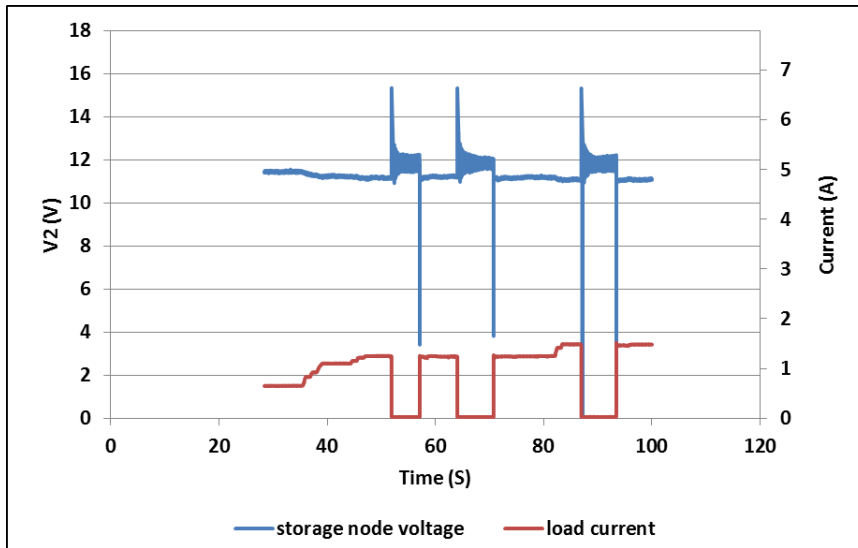


Figure 52: Voltage and Current versus time when a sudden connection/ removal of load occurs on Storage node

From the figure, the load was disconnected after 50s and connected again just before 60s. This is shown by the sudden drop of load current. A huge positive voltage spike of 15V is observed immediately when a 25Ω load is disconnected. As shown in the figure, the storage node immediately shuts down as a result of the high voltage. Connection of the load however leads to a drop in voltage resulting from the in-rush current that gets rectified in milliseconds. The same behaviour occurs for both solar and wind nodes, with the only difference being in the magnitude of the voltage spikes as shown by figure 53 and figure 54 respectively.

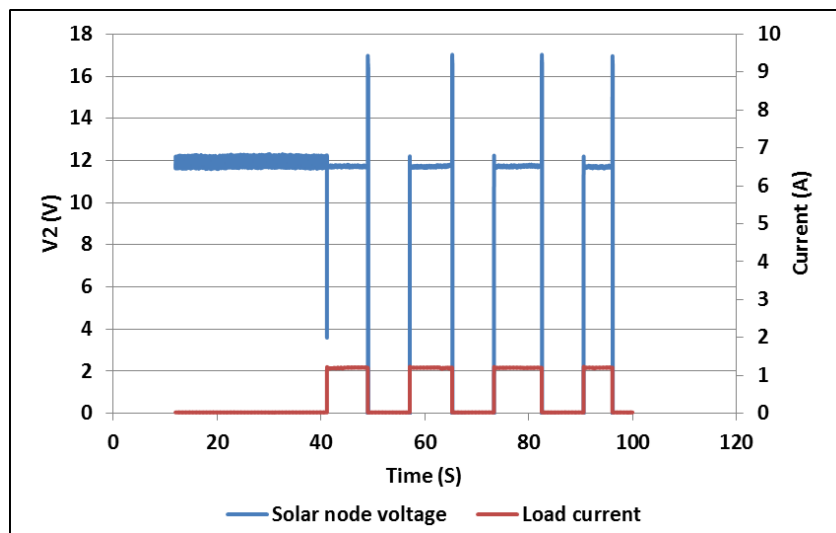


Figure 53: Solar node Voltage and Current versus time from sudden connection/ removal of load

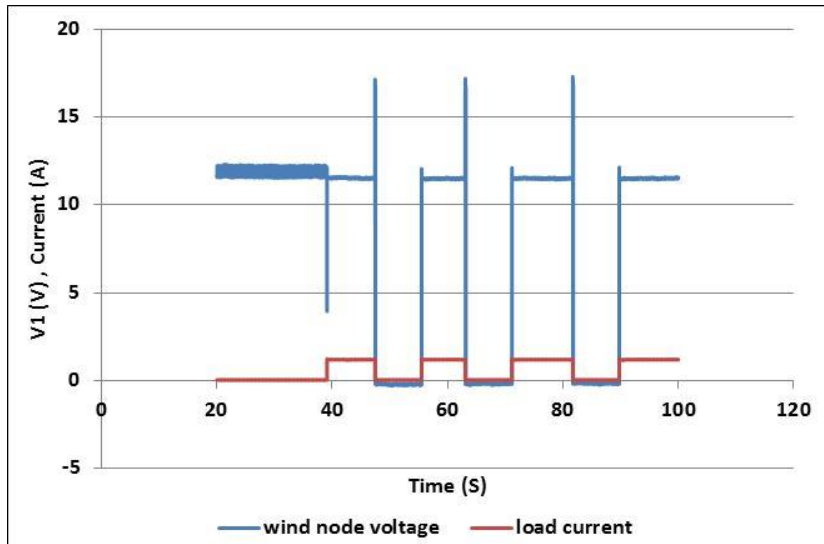


Figure 54: Wind node Voltage and load current versus time from sudden connection/ removal of load

The sudden voltage spikes would however damage electrical circuits if not cleared in the shortest time possible. Additional DC bus capacitors are recommended at each node terminal in order to mitigate the spikes.

7.4. System Tests

System tests were performed by connecting all nodes together and then connecting a variable load at different points on the Picogrid labelled as 1 - 4 in figure 55 below. The main aim of these tests was to prove that a picogrid's power can be scaled up by simply adding more sources or storage nodes. The location of the load within sources and storage nodes also has an effect on the bus voltage at different points on the grid as will be shown. The charging and discharging properties of a storage node were also tested. From figure 55, test case 2, which involves connection of the variable load on the load node terminals, is discussed in this section and the remaining three tests are provided in Appendix O, figure O3, figureO5, figure O6 and figure O7.

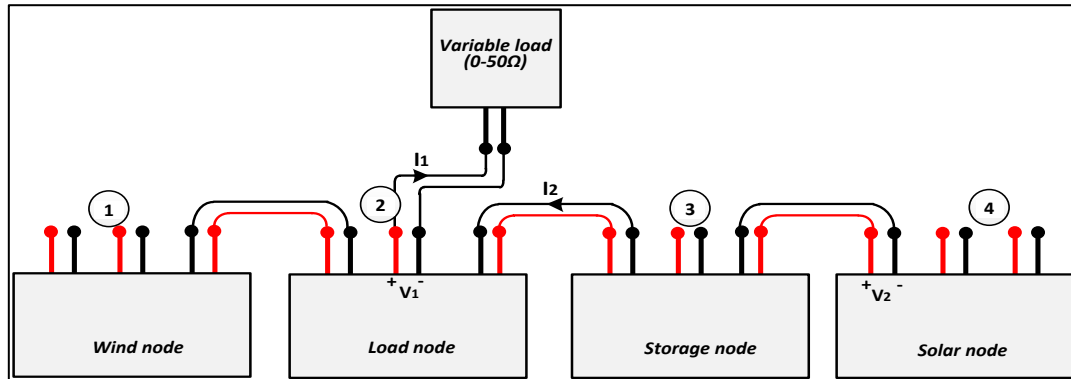


Figure 55: System test setup showing four test cases on four nodes

7.4.1. Load Located on Load Node

From figure 55, a variable load was connected at point 2 and four measurements were recorded graphically whilst varying the resistance with time. The four measurements, V_1 , I_1 , V_2 , I_2 are shown in figure 56 below.

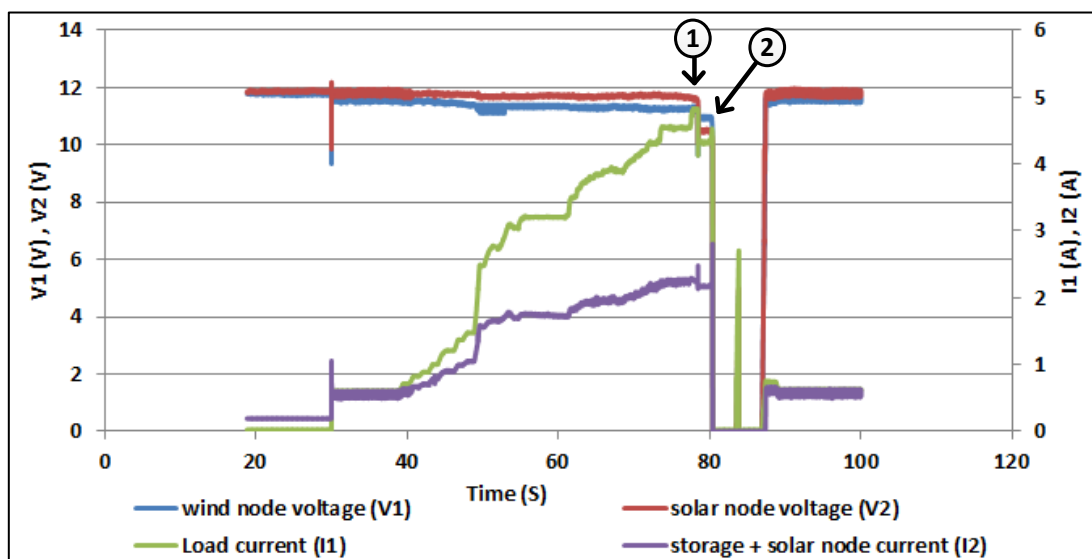


Figure 56: voltages and currents graphs versus time for case 1(on wind node) and case 2 (on load node)

From the figure, a total peak current of **4.95A** was obtained. This gives the picogrid an output power of **59.4W** with just three nodes. Figure 57 shows a more clear voltage versus current graphical presentation of the test case. V_1 was plotted against I_1 and V_2 against I_2 . The points marked 1 on the graphs show the first current threshold point which causes the voltage to drop below the stable region. The second current threshold is reached at point 2 with voltages reaching the critical red zone (under voltage zone) and as a result tripping the node into sleep mode. The reason for having two current thresholds is caused by the storage node's sudden

increase in current that supports the grid and supplies the increasing load for few seconds before finally tripping the node at point 2. The voltages V1 and V2 are not identical due to the distance the solar node is place away from the load node as shown in figure 55.

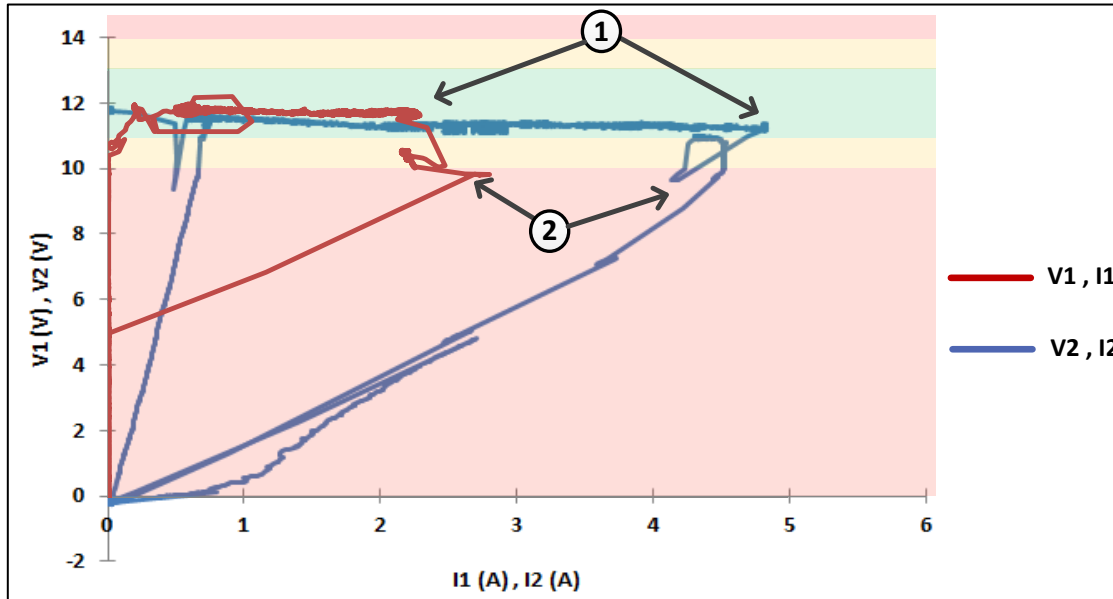


Figure 57: voltage versus current for case 1 and case 2

In order to prove that a picogrid is scalable with just the addition of more sources and storage nodes, the points 1 and 2 will shift to the right as a result of the increase in the supply current. By looking at the previous node tests, figure 42 of a wind node and figure 57 were plotted on the same voltage versus current graph as shown in figure 58 below. The dashed lines show predicted graphs of the Picogrid Bus Voltage (PBV) versus load current when more sources or storage nodes are added. This shows that by adding more sources or storage nodes, a picogrid's power can be easily scaled up whilst trying to achieve stable region (11-13V).

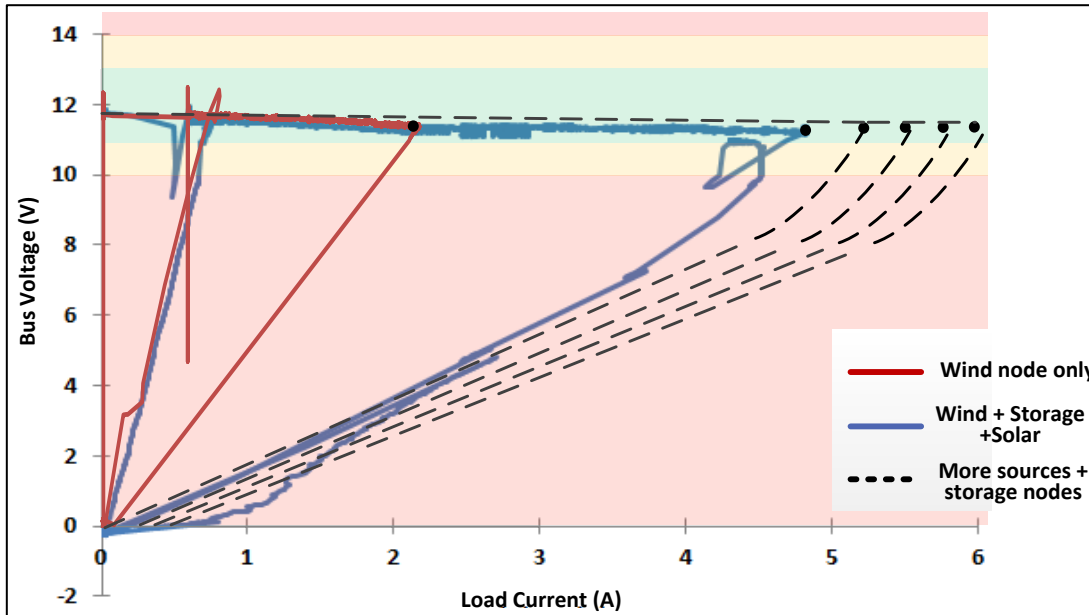


Figure 58: Picogrid voltage versus load current showing how scalability is achieved with additional sources or storage nodes

From the tests above together with all the other cases, a summary of the combined power can be tabulated below.

Table 6: System voltage, current and power ratings of combined two sources and one storage node different cases with varying load

Case (Location of varying load)	Voltage (V)	Current (A)	Power (W)
1 (Wind node)	11.42	3.75	42.8
2 (Load node)	11.54	4.72	54.5
3 (Storage node)	11.18	4.99	55.8
4 (Solar node)	11.31	4.20	47.5

7.4.2. Storage Node test

This test was used to verify the charging properties of a storage node. As described in the previous chapter, a storage node only supports the grid (discharges) when the bus voltage falls below 11.5V. When the bus voltage rises above 13V, the node initiates the charging process. This however can only be visually proved through the use of the HMI display that comes with the node and discussed in the user manual in Appendix F. During the charging process, the HMI display shows the state of battery charge to be increasing as well as providing a charging current for the virtual battery. The discharging process can also be viewed this way but also having voltage and current measurements in a graphical presentation can be useful for verification. Figure 59 shows the test setup with the respective

voltage and current measurements. Current I_2 will be analysed for the storage node charging properties. The graphical presentation of the system is shown in figure 60.

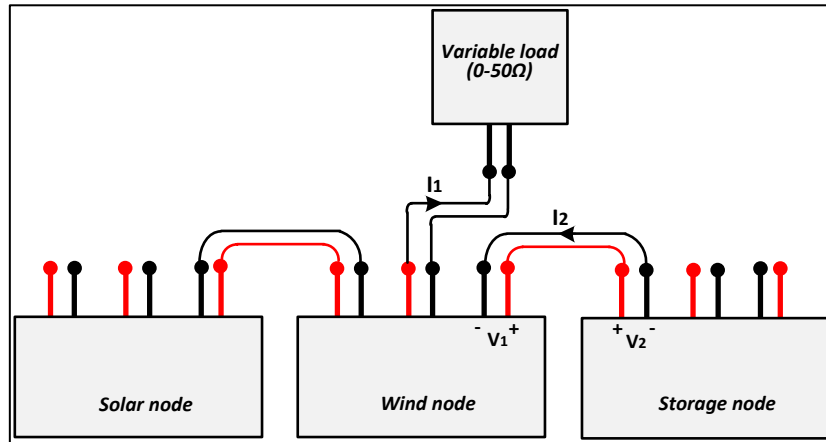


Figure 59: Storage node test setup with two sources

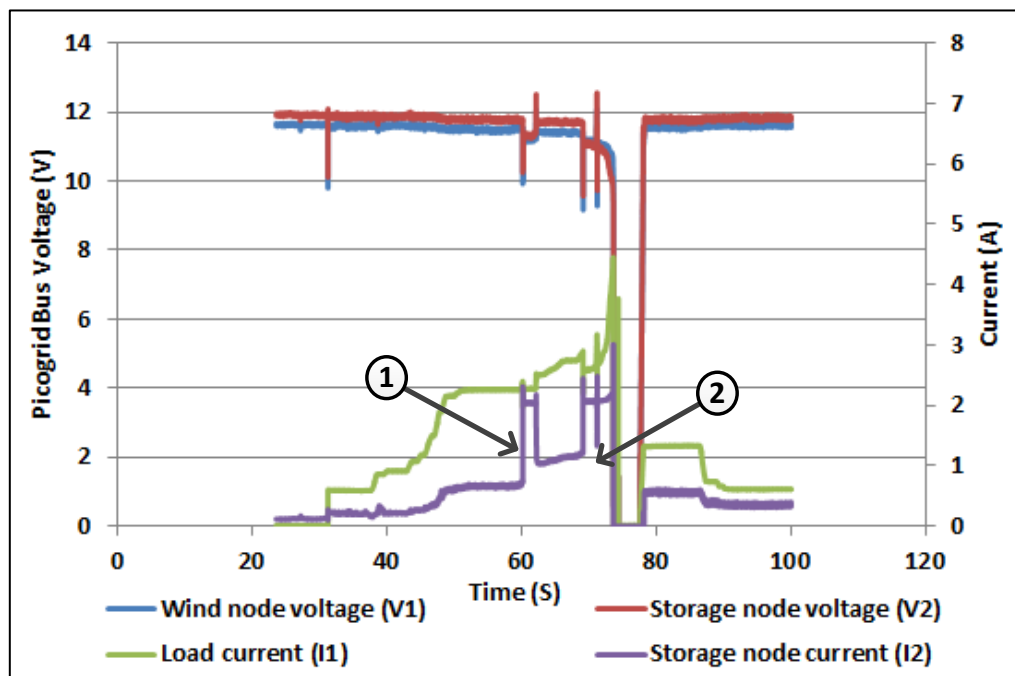


Figure 60: Storage node voltage and current versus time

Region 1 and 2 shown in figure 60 represent the current discharging process of a storage node, which is positive and occurs at 60s and 70s respectively. This is because a storage node's controller is set to discharge power into the grid when the voltage drops below stable region due to a higher load current.

7.5. Summary

This chapter has proved through practical tests that a picogrid is able to withstand different electrical faults resulting from human error or other natural causes. The control algorithm of each node was tested through the different node tests performed together with the overall tests when all nodes were connected together. Accurate electrical specifications of each source and storage node was characterised through the different tests obtained. Some of the unexpected results obtained from the tests such as the undesirable ringing during open circuits can be eliminated through the use of a different control platform. The next chapter provides different recommendations on further tests that can improve the picogrid's operation as well as assisting towards resolving the unexpected results.

8. Conclusion and Recommendations

This chapter summarises the outcomes of this research by answering the research question based on the chapter outcomes. Further recommendations towards the improvement of the Picogrid are also discussed in this chapter.

8.1. Conclusion

This research has proposed a scalable Ad-Hoc Picogrid as a suitable solution for rural electrification compared to other LVDC systems. This has been achieved through a structured engineering approach that first presents a background study of the limitations brought by some of the existing LVDC systems for rural electrification. Secondly, a picogrid is also defined based on the power limits that the system can offer.

Chapter 3 has looked at existing LVDC systems in terms of the structure and methodology behind the centralized control scheme. It was found that the main reason why the systems cannot be scaled up in power is because of the centralized control of voltage and current which makes it difficult for power expansion. A look at the control scheme in LVDC systems showed that only the picogrid uses a similar droop control strategy to that of stand-alone DC microgids. This control of voltage and current is what gives the picogrid the ability to scale up or down the output power.

Chapter 4 then unpacks the picogrid structure and describes its operation. A key feature that has been emphasized on the picogrid concept is the *scalable* nature of the system which simplifies the process of power expansion through the addition of more sources or storage nodes. In order to understand this concept, a detailed explanation of the operation using a “*Grid Code*” has been presented. The grid code provides all the necessary rules based on the picogrid bus voltage that must be obeyed by any node that connects to the picogrid in order to achieve stable operation.

Chapter 5 presents the laboratory implementation of a picogrid prototype by breaking down each node into its hardware composition. The prototype consisting of four nodes (solar, wind, storage and load nodes) was used to apply and test the proposed picogrid concept.

Chapter 6 looks at the control schemes of each node. Three modes of control algorithms have been described as; primary, secondary and tertiary control. The names show the order of

priority that each control occurs so as to ensure that protection to the internal electrical circuitry is maintained in the correct order. Sources and storage nodes apply all the three modes of control whereas a load node only has tertiary control due to the lack of a flyback converter circuit board. Each node's control algorithm was broken down into both analog and digital control schemes with more flexibility offered by the PLC controlled digital control.

Chapter 7 provides the different tests performed on the system. Individual node test were first performed followed by combined system tests. The node tests characterize each node in terms of its power rating and response to sudden open and short circuits as well as over and under voltage levels. The time each node took to recover from these faults was recorded and analysed. Spikes observed on the bus with the sudden removal of a load were minimized by having controllers trip the nodes immediately after the voltage starts to rise. The tests not only prove that a picogrid can self-recover from major electrical faults without any human interaction but also prove the most important aspect of the system being the ease of power scaling through the addition of more sources or storage nodes.

8.1.1. Research Question

The research question was addressed from chapter 5 which compares the older system to the improved control system in chapter 6. The different protection schemes applied to each node utilize the grid code in order to perform the different tasks of fault protection and recovery. The outcome from the test results prove that indeed the protection and control of a picogrid can be improved using the grid code concept.

The different sub-question were answered throughout the document as follows;

Sub-Question 1 - Droop control and PID control were discussed as possible control schemes for a picogrid.

Sub-Question 2 - Scalability is achieved through the addition of nodes as discussed throughout the document with system tests performed to justify this.

Sub-Question 3 - Grid code concept is defined by the bus voltage level states

Sub-Question 4 - Stability and scalability of the picogrid can be improved by having nodes trip in the event of the bus voltage falling out of the stable range (11-13V)

Sub-Question 5 - The grid code can perform well with protection as shown by the test results.

Sub-Question 6 - The grid code is suitable for LVDC as it involves the control of a picogrid at low DC voltage levels.

8.2. Future work Recommendations

The aim of providing future recommendations for this research is so as to give a guideline for future research developments of the Picogrid in both hardware and software aspects. This will further assist in steering the Picogrid concept to a technological solution that can be deployed to the market for use.

8.2.1. Hardware Improvements

The Picogrid concept was tested on one control platform mainly due to the scope limitations of the research and also the availability of the controllers in the research laboratory. The tests performed were thus limited to this platform. It is therefore highly recommended to apply the concept on different control platforms as being done by other fellow research colleagues [53-54] This will assist towards determining the most ideal platform to use as well as offer the flexibility needed in the deployment phase when costs have to be taken into account for a cheaper platform.

The DC-DC converter PCB presents permanent power limitations on how much load it can regulate and thus a complete redesign of the circuit is necessary so as to increase the system's scaling capacity.

The inductor-transformer circuit of the converter needs to be re-designed as well in order to mitigate the voltage spikes as well as

Also having much of the control being done by a digital controller provides more flexibility compared to the analog control presented by the PCB board which requires a completely new PCB printed out.

Source nodes should also be tested using actual PV panels and wind turbines as opposed to the potentiometer controlled regulator knobs in order to analyse the system's performance and ultimately prepare it for deployment.

The node-node interconnection cables for the Picogrid need to be accurately designed in order to cater for the increasing power flow that may result when the nodes are connected in the manner shown in figure 61 below. This is beyond the scope of the research as the choice of the cable will depend on the system size which is determined by the maximum number of nodes allowed for the Picogrid. The maximum power of a picogrid will be clearly determined in the deployment face based on the number of nodes that will be made available for one system. Only after this will one then need to consider the size of the cable which matches the maximum power.

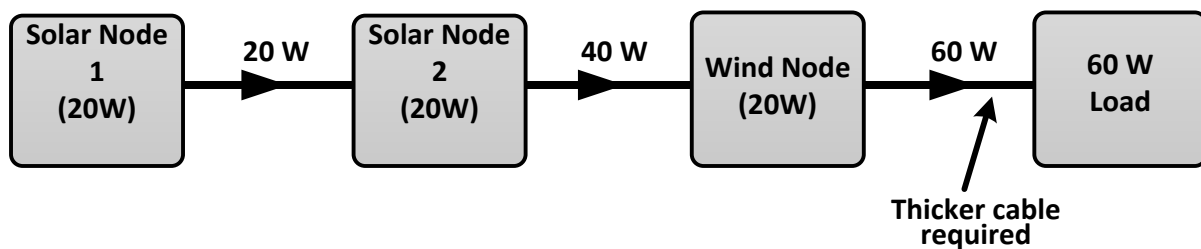


Figure 61: A Picogrid showing limitations with cable properties

8.2.2. Software Improvement

The scope of the research did not include modelling and simulation but rather hardware and software design improvements of the picogrid concept mainly due to time constraints. It is thus recommended to model and simulate the concept on simulation software so as to ease the design process and allow for more tests to be performed before physical implementation. This will bring an added advantage of more simulation tests and flexibility of changing commands without having to modify the physical system.

Also, different control algorithms are recommended for future developments as the research was limited to the droop control that performs a proportional algorithm due to its hardware constraints. Having more advanced control methods such as PID controller will improve the system's response to faults as well as maintaining longer stable operations.

8.2.3. Further Tests

More system tests with regards to different node-node connection topologies need to be conducted in order to find the best topology with maximum efficiency. One of these topologies would be the graph theorem topology defined by graph theory [55]. This would be

the most ideal topology as it provides flexibility whilst limiting the distances between the nodes as shown in figure 62 below. This topology would also reduce costs incurred on the node to node connector cables as the cable thickness requirements would be kept to a minimum. This test can be conducted with as many nodes as possible using software simulations to perform as many tests as possible.

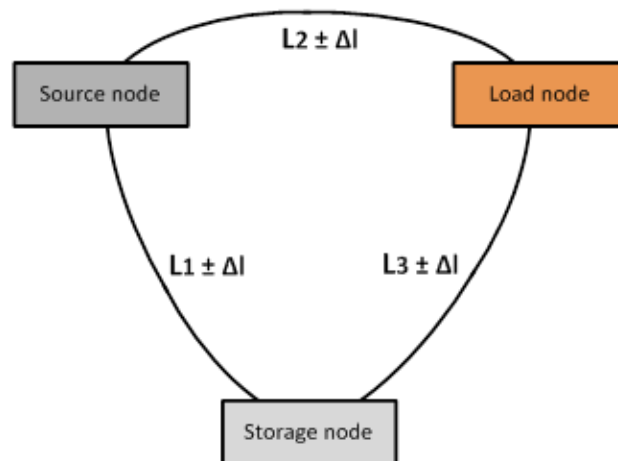


Figure 62: Graph theorem topology approach

Tests on an artificial Grid

An artificial grid such as the one shown in figure 63 could be used in the future to test the different picogrid platforms on one platform for accurate performance comparisons. This artificial grid represents a true 12V battery with fluctuating voltage based on the connected load at the terminals. It will either sink or source current depending on the voltage presented by the node connected at the terminals.

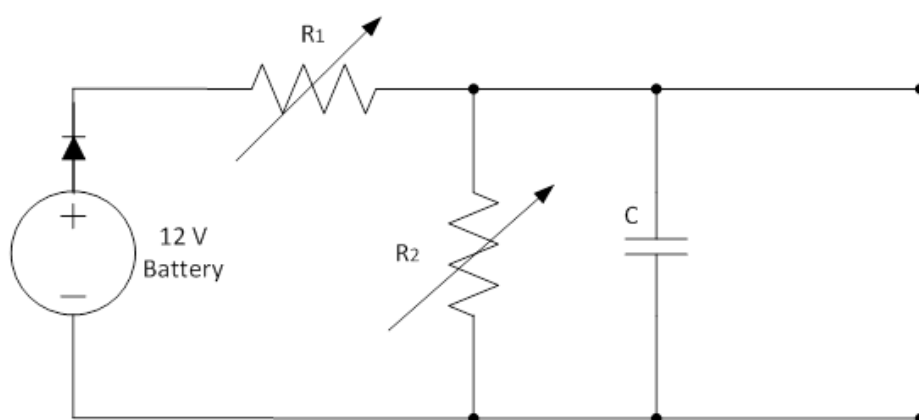


Figure 63: Artificial grid structure

References

- [1] S. K. Ghai, Z. Charbiwala, S. Mylavarapu, D. P. Seetharam , R. Kunnath, "DC Picogrids: A Case for Local Energy Storage for Uninterrupted Power to DC Appliances," *E-Energy, Energy-Efficient Computing and Networking*, pp 27- pp38, January 2013.
- [2] R. Kempener, O. L. D. Saygin, J. Skeer, S. Vinci, and D. Gielen , "Off-Grid Renewable Energy Systems: Status and Methodological Issues," IRENA 2015
- [3] R. Lasseter, A. Akhil, C. Mamay, "Integration of distributed energy resources." *The CERTS Microgrid Concept*, ed, 2002.
- [4] D. Zhaoha, L. Meng, " An Autonomous Operation Microgrid for Rural Electrification," *IEEE conference ESC-228*,pp1-8, 2013.
- [5] International Energy Agency, "World Energy Outlook 2014," OECD/IEA 2014
- [6] International Energy Agency, World Energy Outlook 2016 – Electricity Access Database.
www.worldenergyoutlook.org/media/weowebsite/2015/WEO2016Electricity.xlsx
- [7] U.S Energy Information Administration, *International Energy Outlook 2016-with projections to 2040*,DOE/EIA 0484 |2016|, pp20-63, pp85, May 2016
- [8] AGECC, "Energy for a Sustainable Future," *United Nations – new york*, p7 28 April 2010.
- [9] International Energy Agency, "Africa Energy Outlook," A focus on energy prospects in sub-saharan Africa , p19,p30-39, 2014.
- [10] Mawdsley John, P.Geol, *Renewables vs. Hydrocarbons, The Energy Reality*, AltaCorp Capital, p3-11, April 2011.
- [11] International Energy Agency, "Rural Electrification with PV hybrid systems," IEA-PVPS report, 2013, pp9-15.
- [12] G. A. Villias, "Design of the Human-Powered Generator Module of the Renewable Energy Sharetech Hybrid System," TUDelft, March 2013, pp24-30.
- [13] International Renewable Energy Agency, "Africa's Renewable Future-The path to sustainable Growth," IRENA2013, pp6-10, 2013.
- [14] A. Belward, B. Bisselink, K. Bodis, "Renewable energies in Africa," JRC ST European Commision, 2011, pp7-14, pp43-45.
- [15] International Electrotechnical Commission, "LVDC – The better way," IEC-Geneva, pp3-6, May 2017.
- [16] International Energy Agency, "Rural Electrification with PV hybrid systems," IEA-PVPS report, 2013, pp9-15.
- [17] International Energy Agency, "Africa Energy Outlook," A focus on energy prospects in sub-saharan Africa, p19, p30-39, 2014.
- [18] International Renewable Energy Agency, "Solar PV in Africa: Costs and Market," IRENA- ISBN 978-92-95111-48-6, pp21-24, pp32-34, 2016.

- [19] World Bank Group, "Energy and carbon benefits of pico-powered lighting," *Eco design notes, issue 4*, August 2014.
- [20] J. Hakiri, A. Moyo, G. Prasad, "Assessing the role of solar home systems in poverty alleviation: Case study of Rukungiri district in Western Uganda," *IEEE Conference DUE*, March 2016.
- [21] International Energy Agency, "Pico Solar PV Systems for Remote Homes - A new generation of small PV systems for lighting and communication," *IEA-PVPS report*, pp22-25, 2012.
- [22] Schneider Electric, "Solutions for Access to Energy," *Schneider Electric Industries SAS, version 2*, pp5-10, pp14-16, pp18-20, June 2012.
- [23] SolarNow, "SolarNow Company Profile 2016," SolarNow Services LTD, 2016.
- [24] Phocos, "Pico Solar System," *Phocos AG*, 2014-2015.
- [25] S. K. Ghai, Z. Charbiwala, "Dc picogrids: A case for Local Energy Storage for Uninterrupted Power to DC appliances," IBM research-Radio Studio Chennai, India, May 2013.
- [26] G. A. Villias, "Design of the Human-Powered Generator Module of the Renewable Energy Sharetech Hybrid System," TUDelft, , pp24-30, March 2013.
- [27] K. Strunz, E. Abbasi, D. N. Huu, "DC Microgrid for Wind and Solar Power Integration," *IEEE Trans. Power Electronics*, vol. 2, No.1, pp 116-117, March 2014.
- [28] C. Chan, "DC Microgrids," CSE 291, pp3-7, May 2013.
- [29] D. Qu, M. Wang, Z. Sun, G. Chen, "An Improved DC-Bus Signaling Control Method in A Distributed Nanogrid Interfacing Modular Converters," *IEEE PEDS*, pp214-218, June 2015.
- [30] E. Green, "The iShack: A business model for incrementally upgrading informal settlements," Fact Sheet, April 2013.
- [31] iShack Project: Providing Solar Energy to Under-Served communities
<http://www.ishackproject.co.za/> , Last Accessed 23 June 2017.
- [32] Fenix intl – Bring Power to your Life
<http://www.fenixintl.com/uganda/> , Last Accessed 23 June 2017.
- [33] M. Wiemann, E. María C. Gómez, L. Miró Baz, "Best Practises of the Alliance for Rural Electrification: What renewable energies can achieve in developing and emerging markets," Alliance for Rural Electrification, 3rd edition, pp14, September 2013.
- [34] X. Jianfang, W. Peng, "Multiple Modes Control of Household DC Microgrid with Integration of Various Renewable Energy Sources," *IEEE Industrial Electronics Society, IECON*, pp 1773-pp 1778, 2013.
- [35] S. Kai, Z. Li, X. Yan, and J. M. Guerrero, "A Distributed Control Strategy Based on DC Bus Signaling for Modular Photovoltaic Generation Systems With Battery Energy Storage," *IEEE Transactions on Power Electronics*, vol. 26, pp. 3032 -3045, 2011.
- [36] J. Schonberger, R. Duke, and S. D. Round, "DC -Bus Signaling: A Distributed Control Strategy for a Hybrid Renewable Nanogrid," *IEEE Transactions on Industrial Electronics*, vol. 53, pp. 1453 -1460, 2006.

- [37] Ben S.Yoon, “Exploring the possibilities of Using Used Car Batteries as Residential Energy Storage” MSc Thesis, California State Polytechnic University, Pomona, 2014.
- [38] R. H. Almeida, M. C. Brito, “A review of technical options for solar charging stations in Asia and Africa” AIMS Energy, Volume 3, Issue 3, pp428-449, September 2015.
- [39] G. M. Ponzo, G. Capponi, P. Scalia, V. Boscaino, “An Improved Flyback Converter,” *IEEE Publication*, May 2009.
- [40] A. I. Pressman, K. Billings, T. Morey, “Switching power supply design”. McGraw-Hill, Third edition, pp79-100, pp156-180, 2009.
- [41] K. Billings, T. Morey, “Switch mode power supply handbook,” McGraw-Hill, 3rd Edition, pp294-350, pp , 2011.
- [42] R. Patel and G. Fritz, “Swithing Power Supply Design Review: 60 Watt Flyback Regulator,” Topic 5, Unitrod Corporation, pp 2-20.
- [43] D. Miyimi, R. Robinson, “The Design and Implementation of a Flyback Converter to be Used in a Nanogrid Power System,” School of Elec and Info Engineering, Wits University, 2015.
- [44] ON Semiconductor, “Switch Mode Power supplies – Reference Manual and design guide”, ON Semiconductor, Rev.1, pp20-25 sept 1999.
- [45] *High Speed PWM Controller - UC3825*, Texas Instruments, September 2010
- [46] *SIMATIC S7-1200 Programmable controller system manual*, SIEMENS, pp 15-22, pp 29-70, pp 710-720, April 2012.
- [47] *SITOP PSU100SPower Supply Operating Instructions*, SIEMENS, pp 35-52, August 2014.
- [48] *DC-DC Module Type Regulated Single Output Converter*, SPR01N Series, Mean Well, March 2009.
- [49] *SCALANCE X-Industrial Ethernet Switches*, SIEMENS AG, pp14-20, September 2013.
- [50] S. P. Simpson-Porco, Florian D., F. Bullo, “Stability, Power Sharing, & Distributed Secondary Control in Droop-Controlled Microgrids,” *IEEE international conference on Smart grid communication*, Vancouver, BC, Canada, Dec 2013.
- [51] K. D. Brabandere, B. Bolsens, J. Van den Keybus, A. Woyte, J. Driesen and R. Belmans ,“A Voltage and Frequency Droop Control Method for Parallel Inverters,” *35th IEEE Power Electronics Conference*, Aachen, Germany, pp2501-2507, 2004.
- [52] S. Liu, Y. Zhao, M. Zhao, H. Zhang, “A burst-mode based boost converter harvesting photovoltaic energy for low power applications,” *IEEE Transation*, August 2014.
- [53] M. Aswat, W. Cronje, “Requirements of a Dual Active Bridge for Two Quadrant Power Flow on an Isolated Low Voltage Low Power DC Grid,” MSc. Proposal, EIE, Wits University, Johannesburg, 2017.
- [54] M. R. E. Dangor, W. Cronje, “Exploring the aspects of a digital power solution for a LV-DC Picogrid node,” MSc. Proposal, EIE, Wits University, Johannesburg, 2016
- [55] R. J. Wilson, J. J. Watkins, “Graphs: An Introductory Approach,” John Willey and Sons Inc, , pp 13-24, pp 37-38, pp157-160, 1990.
- [56] *High Stability Isolated Error Amplifier – ADUM3190*, Analog devices, 2013-2015
- [57] *Operating Instructions - Simatic HMI device, KTP400 Basic, KTP600 Basic, KTP1000 Basic, KTP1500 Basic*, SIEMENS Simatic, No.1, Edition 08/2008.

Appendices
